



UNIVERSIDADE ESTADUAL DE CAMPINAS
Faculdade de Engenharia Mecânica

RODOLFO CAVALIERE DA ROCHA

*A Numerical Study on the Combustion of
Ethanol, N-Butanol and their Blends*

*Estudo Numérico da Combustão de Etanol,
N-Butanol e suas Misturas*

CAMPINAS
2016

RODOLFO CAVALIERE DA ROCHA

***A Numerical Study on the Combustion of
Ethanol, N-Butanol and their Blends***

***Estudo Numérico da Combustão de Etanol,
N-Butanol e suas Misturas***

Thesis presented to the School of Mechanical Engineering of the University of Campinas in partial fulfillment of the requirements for the degree of Master in Mechanical Engineering, in the area of Thermal and Fluid Engineering.

Dissertação apresentada à Faculdade de Engenharia Mecânica da Universidade Estadual de Campinas como parte dos requisitos exigidos para obtenção do título de Mestre em Engenharia Mecânica, na Área de Térmica e Fluidos.

Orientador: Prof. Dr. Rogério Gonçalves dos Santos

ESTE EXEMPLAR CORRESPONDE À VERSÃO FINAL DA DISSERTAÇÃO DEFENDIDA PELO ALUNO RODOLFO CAVALIERE DA ROCHA, E ORIENTADO PELO PROF. DR. ROGÉRIO GONÇALVES DOS SANTOS.

.....
ASSINATURA DO(A) ORIENTADOR(A)

**CAMPINAS
2016**

Agência(s) de fomento e nº(s) de processo(s): CAPES, 33003017

Ficha catalográfica
Universidade Estadual de Campinas
Biblioteca da Área de Engenharia e Arquitetura
Luciana Pietrosanto Milla - CRB 8/8129

R582n Rocha, Rodolfo Cavaliere da, 1990-
A numerical study on the combustion of ethanol, n-butanol and their blends
/ Rodolfo Cavaliere da Rocha. – Campinas, SP : [s.n.], 2016.

Orientador: Rogério Gonçalves dos Santos.
Dissertação (mestrado) – Universidade Estadual de Campinas, Faculdade
de Engenharia Mecânica.

1. Combustão. 2. Cinética química. 3. Etanol. 4. Butanol. I. Santos, Rogério
Gonçalves dos, 1978-. II. Universidade Estadual de Campinas. Faculdade de
Engenharia Mecânica. III. Título.

Informações para Biblioteca Digital

Título em outro idioma: Estudo numérico da combustão de etanol, n-butanol e suas misturas

Palavras-chave em inglês:

Combustion
Chemical kinetics
Ethanol
Butanol

Área de concentração: Térmica e Fluídos

Titulação: Mestre em Engenharia Mecânica

Banca examinadora:

Rogério Gonçalves dos Santos [Orientador]
Waldir Antonio Bizzo
Amir Antônio de Oliveira Júnior

Data de defesa: 13-07-2016

Programa de Pós-Graduação: Engenharia Mecânica

UNIVERSIDADE ESTADUAL DE CAMPINAS
FACULDADE DE ENGENHARIA MECÂNICA
COMISSÃO DE PÓS-GRADUAÇÃO EM ENGENHARIA MECÂNICA
DEPARTAMENTO DE ENERGIA

DISSERTAÇÃO DE MESTRADO ACADÊMICO

*A Numerical Study on the Combustion of
Ethanol, N-Butanol and their Blends*

*Estudo Numérico da Combustão de Etanol,
N-Butanol e suas Misturas*

Autor: Rodolfo Cavaliere da Rocha

Orientador: Prof. Dr. Rogério Gonçalves dos Santos

Coorientador:

A Banca Examinadora composta pelos membros abaixo aprovou esta Tese:

Prof. Dr. Rogério Gonçalves dos Santos, Presidente
UNICAMP/FEM

Prof. Dr. Waldir Antonio Bizzo
UNICAMP/FEM

Prof. Dr. Amir Antônio Martins de Oliveira Júnior
UFSC/CTC/EMC

A Ata da defesa com as respectivas assinaturas dos membros encontra-se no processo de vida acadêmica do aluno.

Campinas, 13 de julho de 2016.

Dedication

To the Brazilian and Paraguayan people, to whose sons and daughters the achievements in science and technology are more than mere results. They are miracles.

Acknowledgments

I would like to thank some people and entities without whom I would not be able to accomplish this task.

Firstly, I would like to thank my advisor for all the support in every step of my work, specially for keeping me interested in the subject even in the hardest times. It would be hard to enumerate everything he helped me with in all that time, but I can affirm, without a shadow of doubt, that if it was not for his help nothing would have been done. To have Professor Rogério dos Santos by my side was a privilege.

Secondly, I would like to thank our international research group, specially Professor Darabiha, from the EM2C (France) and Professor Alviso, from FIUNA (Paraguay). The first for all the help with the software used in the project, as well as for helping me understand what was possible and what was impossible to do, and the latter, for his strong contribution to my work, acting as an unofficial co-advisor. He has also received me and my colleague, Marina, in his laboratory in FIUNA for a research internship, having even ceded a room in his own home for a night before we find a place to stay.

I would also like to thank the University of Campinas for providing what I needed for my project, the National University of Asunción, in Paraguay, for providing the means for my internship, and the EM2C/CentraleSupélec, in France, for ceding the package used in my research.

I am also thankful for my family and friends for all the help in keeping me focused, and for the relaxation moments. I would like to thank Marina, my colleague, for all the help and company during our research. Finally, my special acknowledgment goes to Laura, my girlfriend, who helped me focus, gave me strength and made me understand my personal mission.

I cannot forget to mention the members of the defense board, for their interest in my project and for their valuable contribution to the final work. They have the experience of a lifetime in combustion, knowing even a couple of curious facts on the research in the field. With their tips and advices I could not only tremendously improve the quality of this text, but also better understand the difficulties related to the subject; for that I am very grateful.

Lastly, I would like to thank CAPES for financing the scholarship, crucial for the progress of the project.

*The only place where success comes
before work is in a dictionary.*

unknown author

Resumo

O álcool n-butanol é uma substância orgânica que tem sido proposta como combustível alternativo para motores à combustão interna. Melhorias em seu processo de produção como biocombustível, por meio de processos de fermentação ABE, a partir da biomassa, chamam a atenção para sua sustentabilidade econômica e ambiental; por outro lado, suas características físico-químicas e de queima, próximas à da gasolina e do diesel comerciais, sugerem seu uso combinado ou como substituto dos mesmos. Apesar disso, ainda se sabe pouco acerca das características de sua combustão, motivando a pesquisa na área. O etanol, por sua vez, é um biocombustível extensamente utilizado em motores de ciclo Otto, principalmente no Brasil e nos Estados Unidos, sendo produzido por processos eficientes de fermentação, inclusive como subproduto da produção de butanol no processo ABE; por suas características físico-químicas, de produção e queima, propõe-se que seja misturado ao n-butanol em aplicações comerciais. O presente estudo compara esquemas de cinética química da queima em ar de n-butanol e etanol, entre si e em relação a dados experimentais disponíveis na literatura, por meio da simulação de chama laminar unidimensional pré-misturada no pacote REGATH (EM2C/CNRS - França). Em seguida, um novo esquema combinado é desenvolvido, que apresenta boa concordância com resultados experimentais da literatura para ambos os combustíveis nessas condições. Por fim, são levantadas curvas características da chama de misturas entre os compostos em diversas proporções, que poderão ser comparadas com dados experimentais em futuros trabalhos.

Palavras-chave: Combustão, Cinética Química, Etanol, Butanol.

Abstract

The alcohol n-butanol is an organic substance being proposed as an alternative fuel for internal combustion engines. Improvements in its production as a biofuel, through ABE fermentation processes, grow attention for its economic and environmental sustainability; on the other hand, its physicochemical and burning characteristics, close to those of commercial gasoline and diesel, suggest its usage as an additive or a substitute fuel. However, relatively few is known about its combustion characteristics, thus motivating research in that area. Ethanol, instead, is a biofuel widely used in Otto engines, especially in Brazil and the United States, being produced by efficient fermentation processes, and is occasionally a by-product of the butanol formation (ABE process); due to its physicochemical, burning and production characteristics, the addition of this fuel to butanol in commercial applications is proposed. The present study compares chemical kinetic schemes for the burning on air of n-butanol and ethanol, between each other and against experimental data available in the literatures, through simulations in one-dimensional premixed flame configuration in the REGATH package (EM2C/CNRS - France). Further, a new combined scheme is developed, presenting good agreement with experimental results from the literature for both fuels in these conditions. In the end, theoretical data for the flame of mixtures between these substances is raised, in different blending proportions, which might be compared with results from experiments to be run in future projects.

Keywords: Combustion, Chemical Kinetics, Ethanol, Butanol.

List of Figures

1.1	Global ethanol production by country. Source: AFDC (2016)	16
1.2	Sketch of phase diagram for the ternary system of acetone (ethanol)–butanol–water at 298 K: (I) heterogeneous area and (II) homogeneous area; the fractions of acetone: ethanol are all weight fraction. Adapted from Zhou <i>et al.</i> (2014)	19
2.1	Laminar flame structure. Source: Turns (2012).	27
2.2	(a) Bunsen-burner schematic. (b) Laminar flame speed equaling the normal component of the unburned gas velocity, $v_{u,n}$. Source: Turns (2012).	39
2.3	(a) Adiabatic flat-flame burner. (b) Non-adiabatic flat-flame burner. Source: Turns (2012).	40
2.4	Constant-volume spherical bomb	41
2.5	Laminar flame speed for ethanol, n-butanol and iso-octane. Adapted from Broustail <i>et al.</i> (2011).	46
3.1	Graphic representation of the fusion of kinetic schemes.	58
4.1	Laminar flame speed of n-butanol/air combustion from various works, $T = 353K$, $p = 1atm$. * Values from Sarathy <i>et al.</i> (2009) were evaluated at $T = 350K$ and $p = 0.89atm$	60
4.2	Laminar flame speed of ethanol/air combustion from various works, $T = 298K$, $p = 1atm$	61
4.3	Relation between laminar flame speeds for blends and that of pure ethanol, evaluated through the scheme from Sarathy <i>et al.</i> (2012), $T = 298K$, $p = 1atm$	63
4.4	Laminar flame speed of n-butanol/air combustion from previous analysis and the new scheme, $T = 353K$, $p = 1atm$. * Values from Sarathy <i>et al.</i> (2009) evaluated at $T = 350K$ and $p = 0.89atm$	64
4.5	Laminar flame speed of ethanol/air combustion from previous analysis and the new scheme, $T = 298K$, $p = 1atm$	65
4.6	Relation between laminar flame speeds for blends and that of pure ethanol, evaluated through the new scheme, $T = 298K$, $p = 1atm$	66
4.7	Temperature profile for B100 and E100, $T_0 = 298K$, $p = 1atm$	68
4.8	Mass fraction of O_2 , $T_0 = 298K$, $p = 1atm$	68
4.9	Mass fractions of pure fuels (ethanol and n-butanol), $T_0 = 298K$, $p = 1atm$	69
4.10	Mass fraction of H_2O , $T_0 = 298K$, $p = 1atm$	69
4.11	Mass fraction of CO_2 , $T_0 = 298K$, $p = 1atm$	70
4.12	Mass fraction of CO , $T_0 = 298K$, $p = 1atm$	70
A.1	Coordinate systems for planar flames, spherically symmetric flames (droplet burning) and axysymmetric flames (jet flames). Source: Turns (2012).	80

List of Tables

1.1	Specification of alcohols and conventional fossil fuels. Adapted from Jin <i>et al.</i> (2011)	15
1.2	Molecular structure and main application of butanol isomers. Adapted from Jin <i>et al.</i> (2011).	17
2.1	Recommended rate coefficients for $H_2 - O_2$ reactions. Adapted from Turns (2012 apud. Warnatz, 1984)	25
2.2	Comparison between laminar flame speed works for n-butanol and ethanol combustion	47
B.1	Laminar Flame Speed for Models and Experiments for N-Butanol, $T = 353K$, $p = 1 atm$	87
B.2	Laminar Flame Speed for Models and Experiments for Ethanol, $T = 298K$, $p = 1 atm$	88
B.3	Laminar Flame Speed for Blends through the scheme from Sarathy <i>et al.</i> (2012), $T = 298K$, $p = 1 atm$	89
B.4	Laminar Flame Speed for Blends through the new scheme, $T = 298K$, $p = 1 atm$	89
B.5	Standard Deviation for Ethanol Models, in cm/s	90
B.6	Standard Deviation for N-Butanol Models, in cm/s	90

Summary

1	INTRODUCTION	14
1.1	Ethanol	15
1.2	N-Butanol	17
1.3	Blending of Ethanol and N-Butanol	18
1.4	Objectives	19
1.5	Work Structure	20
2	LITERATURE REVIEW	21
2.1	Chemical Kinetics	21
2.2	One-Dimensional Laminar Premixed Flame	26
2.2.1	Main Characteristics	27
2.2.2	Flame Analysis	29
	Considerations	29
	Continuity	30
	Species Conservation	30
	Energy Conservation	30
2.3	Auxiliary Properties	31
2.3.1	Thermodynamic Properties	32
2.3.2	Transport Properties	34
	Viscosity	35
	Binary Diffusion Coefficient	35
	Thermal Conductivity	37
2.4	Common Laminar Premixed Laboratory Flames	39
2.5	State-of-the-Art	42
2.5.1	Kinetic Schemes	42
	N-Butanol	42
	Ethanol	43
2.5.2	Experimental Data	44
	N-Butanol	44
	Ethanol	45
	N-Butanol and Ethanol Studies	45
2.6	Summary of the Works on Ethanol and N-Butanol	46
3	METHODOLOGY	50
3.1	Numerical Simulation Parameters	50
3.1.1	Target Data	50

3.1.2	Flame Set	51
3.1.3	Initial Temperature and Pressure	51
3.1.4	Fuel-Air Equivalence Ratios	52
3.1.5	REGATH	52
3.2	Comparison between Kinetic Schemes and Experimental Data	54
3.3	Blends Simulation through Scheme for Butanol Isomers	55
3.4	Development and Validation of Combined Scheme for Ethanol + N-Butanol . .	55
3.5	Blends Simulation through the New Scheme	59
4	RESULTS AND DISCUSSION	60
4.1	Comparison between Kinetic Schemes and Experimental Data	60
4.2	Blends Simulation through Scheme for Butanol Isomers	62
4.3	Development and Validation of Combined Scheme for Ethanol + N-Butanol . .	63
4.4	Blends Simulation through the New Scheme	66
5	CONCLUSIONS AND FUTURE WORK PERSPECTIVES	72
5.1	Conclusions	72
5.2	Future work perspectives	73
	Bibliography	75
	APPENDICES	80
A	– Conservation Equations for Laminar Reacting Flows	80
A.1	Mass Conservation	81
A.2	Species Conservation	82
A.3	Momentum Conservation	83
A.4	Energy Conservation	85
B	– Tables	87
B.1	Laminar Flame Speed	87
B.2	Standard Deviation for Schemes	90

1 INTRODUCTION

Biofuels are defined as flammable substances in some way derived from biomass, used to generate energy through their combustion (Jin *et al.*, 2011). In this category can be included any fuel produced from seeds, fruits, bagasse or any other biological sources. They can be considered renewable, which means their sources can be renewed in a human-life scale (El-labban *et al.*, 2014). It is also interesting from the point of view of greenhouse effect emissions, considering that a great part of the CO_2 emitted is captured in the feedstock production process. They are considered as some of the most promising energy sources for the future, specially, but not limited to, transportation purposes. Uncertainties related to the availability of petrol reserves, prices fluctuations related to political and economical instabilities, as well as the interest in reducing greenhouse gases emissions drive attention to this field.

According to the *Key World Energy Statistics 2015* (IEA, 2015), 81.4% of the global primary energy supply comes from fossil fuels, specially those derived from petrol, responsible for 31.1% of the total amount. 63.8% of the petrol consumed worldwide is used in transportation, and its products are responsible for 92.6% of the total energy consumed by vehicles, attesting the extreme dependency to this source. Biofuels, on the other hand, represent only 2.5% of the total, fraction that might rise depending on the developments in the production and burning technologies, as well as their commercial application. Considering only CO_2 emissions, the most important greenhouse effect gas, petrol-derived fuels are responsible for 33.6% of the global number, fraction only lower than that of coal. Biofuels, despite producing CO_2 when burned, recapture that amount in the production process, being consumed during the plants' growth.

Brazil is one of the leaders in the development and usage of biofuels. Historically, it was the first to use bioethanol at commercial level, during the 1970's oil crisis. The *ProAlcool*, or *Programa Nacional do Alcool* (National Alcohol Program), was established in order to prevent a slow down effect on energy consumption and, consequently, in the economy (Rosillo-Calle and Cortez, 1998). From then to now, about 80% of the vehicles in use in Brazil run blends between ethanol and gasoline, being mandatory for commercial gasoline to be sold with a minimum of about 20% of alcohol in volume, in a rate defined by governmental policies. A great part of the cars sold in the country present flex-fuel engines, prepared to run both gasoline and ethanol in any proportion (Su *et al.*, 2015). Biodiesel, defined in Brazilian law no. 11.097/2005

as any biomass-based fuel that can be used in compression-ignition engines, are also widely used, and the addition of a certain amount of it in commercial diesel sold in the local market is also mandatory. Apart from that, aviation biofuels are also being developed, in international cooperation (Su *et al.*, 2015).

Among biofuels, alcohols produced by fermentation processes, like bioethanol and biobutanol, present characteristics that suggest their suitability in vehicles, specially in spark-ignition engines. They present themselves in liquid form at room temperatures, they are relatively easy to produce and, like petrofuels, they have high energy density (Bergthorson and Thomson, 2015). They also present high octane number, crucial for that kind of engine (Heywood, 1988). Table 1.2 presents those and other physicochemical characteristics.

Table. 1.1: Specification of alcohols and conventional fossil fuels. Adapted from Jin *et al.* (2011)

	Gasoline	Diesel	Methanol	Ethanol	n-Butanol
Molecular formula	$C_4 - C_{12}$	$C_{12} - C_{25}$	CH_3OH	C_2H_5OH	C_4H_9OH
Cetane number	0-10	40-55	3	8	25
Octane number (RON)	80-99	20-30	111	108	96
Oxygen content (% weight)	-	-	50	34.8	21.6
Density (g/ml) at 20°C	0.72-0.78	0.82-0.86	0.796	0.790	0.808
Autoignition temperature (°C)	300	210	470	434	385
Flash point (°C) at closed cup	-45 to -38	65 to 88	12	8	35
Lower heat value (MJ/kg)	42.7	42.5	19.9	26.8	33.1
Boiling point (°C)	25-215	180-370	64.5	78.4	117.7
Stoichiometric air/fuel mass ratio	14.7:1	14.3:1	6.49:1	9.02:1	11.21:1
Latent heating (kJ/kg) at 25°C	380-500	270	1109	904	584
Flammability limits (%vol.)	0.6-8	1.5-7.6	6.0-36.5	4.3-19	1.4-11.2
Saturation pressure (kPa) at 38°C	31.01	1.86	31.69	13.8	2.27
Viscosity (mm ² /s) at 40°C (20°C)	0.4-0.8	1.9-4.1	0.59	1.08	2.63

1.1 Ethanol

Ethanol (C_2H_5OH) is perhaps the liquid alternative fuel most widely studied (Demirbas, 2007). In vehicles, it is mainly used as a fuel additive, specially when blended with

gasoline to enhance its octane number and improve combustion in spark-ignition engines, but also as a renewable alternative fuel, specially in Brazil (Agarwal, 2007). Its advantages for this application are the high octane number, the low cetane number and the easiness of blending with other fuels. On the other hand, ethanol is corrosive to common pipelines through general, dry and wet corrosion, due to ionic impurities, to the polarity of the ethanol molecule and to the water contained in the fuel or from the moisture absorbed from the atmosphere, respectively. Additionally, its energetic density is lower than that of gasoline, requiring more liters of fuel to run the same distances (Jin *et al.*, 2011).

As previously cited, it is produced in commercial levels since the 1970's in Brazil (Rosillo-Calle and Cortez, 1998), and nowadays its production accounts for more than 25.682 billion gallons (AFDC, 2016). It is mainly produced from the fermentation of sugar from sugar cane, in Brazil, and from that of corn starch, in the United States, in the so-called first-generation processes, which use edible feedstock. Second-generation processes, on the other hand, produce ethanol from inedible feedstock, such as lignocelluloses, and are being developed worldwide (Dias *et al.*, 2012). Those traditional production processes mainly generate ethanol and water, however, this fuel can also be formed in ABE processes, which consist in the generation of acetone, n-butanol and ethanol through bio-reactors using bacteria of the genus *Clostridium*. ABE processes can be adjusted for different yields of each component (Jin *et al.*, 2011).

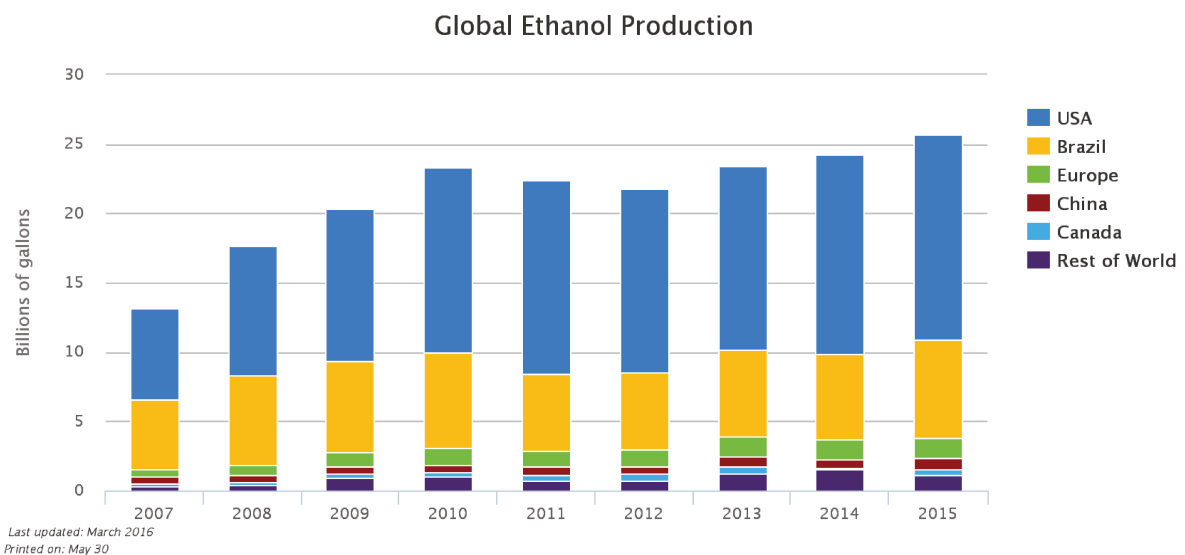

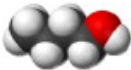
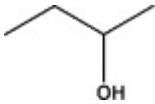
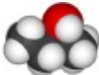
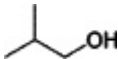

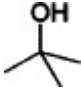
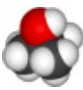


Figure. 1.1: Global ethanol production by country. Source: AFDC (2016)

1.2 N-Butanol

N-Butanol is one of the four butanol isomers, a group of alcohols described by the formula C_4H_9OH . Details of its isomers are presented in table 1.2.

Table. 1.2: Molecular structure and main application of butanol isomers. Adapted from Jin *et al.* (2011).

Butanol isomer	Molecular structure	Sketch map	Main applications
1-Butanol			Solvents for paints, resins, dyes, etc. Plasticizers to improve plastic material processes Chemical intermediate for butyl esters or butyl ethers, etc. Cosmetics , including eye makeup, lipsticks, etc. Gasoline additive
2-Butanol			Solvent Chemical intermediate for butanone, etc. Industrial cleaners , such as paint removers Perfumes or in artificial flavors
iso-Butanol			Solvent and additive for paint Gasoline additive Industrial cleaners , such as paint removers Ink ingredient
tert-Butanol			Solvent Denaturant for ethanol Industrial cleaners , such as paint removers Gasoline additive for octane booster and oxygenate Intermediate for MTBE, ETBE, TBHP, etc.

N-Butanol is the normal isomer of the group, presenting the radical OH^- in the end of the carbon chain. Its main application is as intermediate in chemical processes, but is recently being proposed as a renewable alternative fuel, as well as additive for gasoline in spark-ignition

engines or even for diesel in compression-ignited engines. Its main advantages for the first are the octane number close to that of commercial gasoline, better energy density (meaning better mileage than ethanol) and lower interaction with engine parts. However, its cetane number is higher than that of both ethanol and gasoline, indicating possible auto-ignition problems when used solely in that application, for example - despite being an interesting characteristic for diesel engines, something also being researched. Nowadays, unfortunately, the most significant disadvantage of n-butanol is the fact that its production processes cannot yet compete with those of other commercial fuels, both in terms of costs and yield, requiring improvements in order to become economically viable (Jin *et al.*, 2011).

Commercially, its most common production process involves processing of petrol, but improvements in the ABE processes, specially in its yield, lead to increase in the production of n-butanol from biomass, the so-called biobutanol. As previously explained in section 1.1, ABE fermentation involves bacteria of the genus *Clostridium*, generating a mixture of acetone, n-butanol and ethanol, as well as water and other impurities Jin *et al.* (2011). Depending on the species employed, this process can use edible or non-edible feedstock. By genetically changing the bacteria involved it is possible to adjust ABE fermentation to a range of proportions between its main products Jin *et al.* (2011). In Brazil, there are also studies being conducted involving the generation of n-butanol from ethanol in sugar refineries (Dias *et al.*, 2014), which may grow interest in its local application.

1.3 Blending of Ethanol and N-Butanol

Considering the complementary characteristics presented by ethanol and n-butanol, namely the higher octane number and lower cetane number of the first and the better chemical stability and higher energy density of the latter, as well as the fact that they can be produced together in ABE processes, its combined use is suggested. Recent studies also indicate that both fuels are perfectly soluble, at least at room temperature (figure 1.2, phase diagram), which reinforces the idea of using their blends in engines (Zhou *et al.*, 2014).

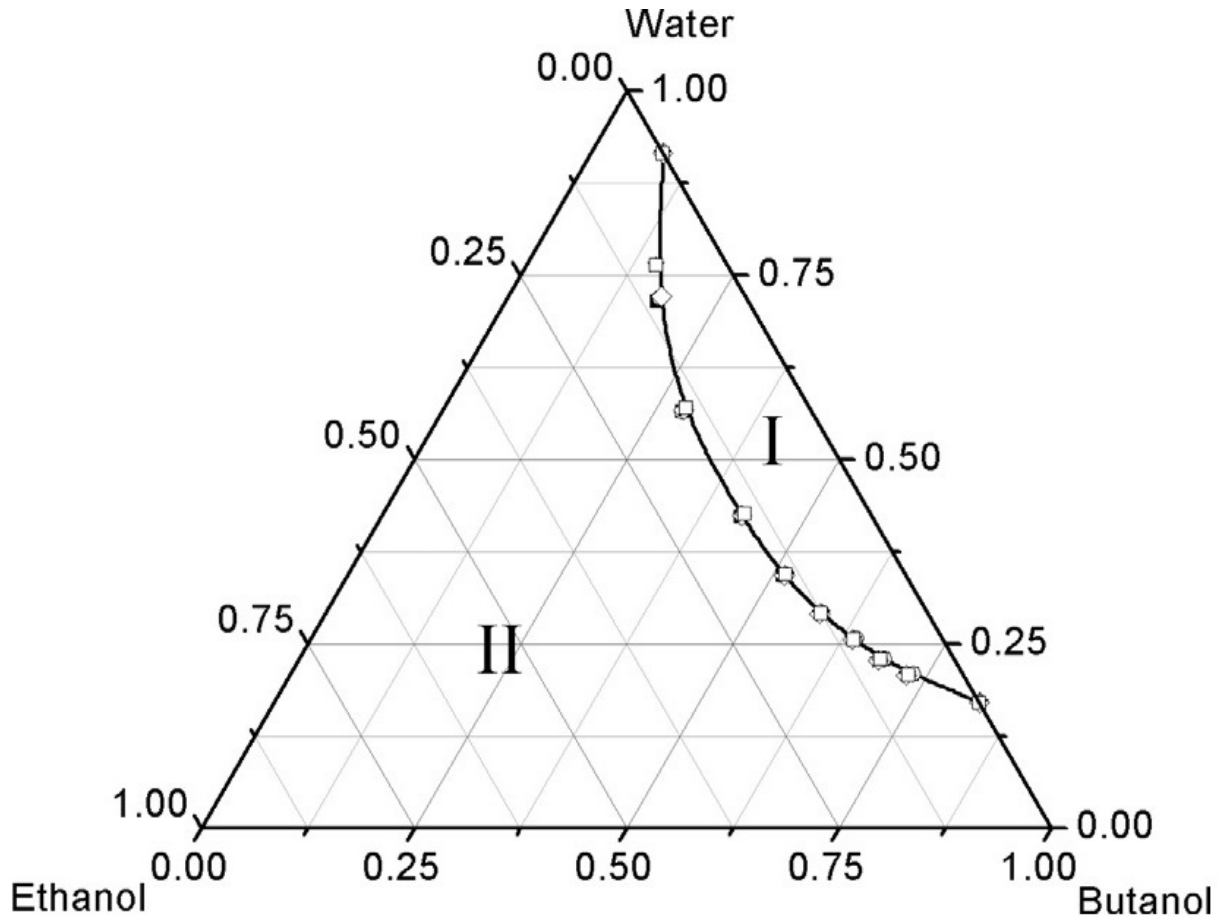


Figure. 1.2: Sketch of phase diagram for the ternary system of acetone (ethanol)–butanol–water at 298 K: (I) heterogeneous area and (II) homogeneous area; the fractions of acetone: ethanol are all weight fraction. Adapted from Zhou *et al.* (2014)

In order to define the behavior of the combustion of these blends, studies involving chemical kinetics and burning characterization are necessary, both for laminar and turbulent sets, in order to create a basis to be used to describe how it would happen in real engines, helping the development of the usage of these alternative fuels.

1.4 Objectives

The present work intends to study the behavior of the laminar combustion of mixtures between n-butanol and ethanol on air, in different fuel proportions. In order to do it, the package REGATH, developed by the laboratory EM2C (CNRS - CentraleSupélec), in France, was used. In this application the burning of these blends was simulated in an one-dimension laminar premixed flame configuration. Chemical kinetic schemes and experimental data available

in the literature were compared, further developing a fused scheme, capable of describing the combustion of each of the fuels, when compared to experiments of previous works. The studied characteristics were the laminar flame speed and the mass fraction of selected chemical species for several fuel/air equivalence ratios. In the end, curves for blends containing 25, 50 and 75% in volume of n-butanol in ethanol, describing these characteristics, were raised.

1.5 Work Structure

The present work is divided in five chapters.

The first chapter introduces the subject of the project, presenting ethanol and n-butanol in their most recently known characteristics, as well as information on their production and usage. This chapter also explains why the blends between both fuels were studied, and the objectives of this study.

The second chapter presents a bibliographic review of the theory related to the present study, explaining chemical kinetics and involved properties. This section also presents state-of-the-art kinetic schemes and experiments done for both fuels, bringing a comparative between their characteristics.

The third chapter explains the methodology used in the project, describing the steps done in the course of the work, the software used, the numerical configuration and other details. The comparison between kinetic schemes and experimental data is described, as well as the development of the combined scheme and the data raised for blends.

The fourth chapter describes the work done and its results, presenting curves for the chemical schemes available in the literature, for the combined one and the experiments of previous studies, showing the main data raised for ethanol, n-butanol and their blends. In the end of the chapter these results are analyzed and discussed.

The fifth chapter presents the conclusions of the present work, summarizing the whole study and raising further questions to be answered. In the end, suggestions for future works involving the subject are given.

2 LITERATURE REVIEW

Combustion is defined generically as a chemical process in which a rapid oxidation occurs, generating heat, or both light and heat (Turns, 2012). The science of combustion is very complex, and involves subjects as varied as chemical kinetics, fluid mechanics and thermodynamics. It is impossible to fully understand and fully control the phenomenon, however, for most practical applications there are ways of evaluating its characteristics numerically and experimentally.

The present work involves a certain field of the combustion science known as Chemical Kinetics. Through this literature review, this chapter intends to describe the concepts related to this area, also giving a brief explanation on the thermodynamic and transport properties. Other concepts related to the studied flame set and its characteristics are also described. In the end, the state-of-the-art in chemical schemes for ethanol and n-butanol is presented, ending with table 2.2, which represents all the evaluated works.

2.1 Chemical Kinetics

Chemical kinetics is the name given to the science of the elementary reactions and their rates, a specific branch of the physicochemistry. Its theory is explained in details in the works of Turns (2012) and Darabiha *et al.* (2006). For the combustion science this study is of fundamental importance, considering it defines pollutant formation, produced heat, flame speed, temperatures, among other characteristics of the burning process. Progress in this field is responsible for a great part of the development of the combustion in the present days, considering that it bases the computer simulation of reactant systems (Turns, 2012).

For many thermodynamic applications, it is enough to use only the global reaction, which considers only the reactants and the main final products. However, real combustion processes involve thousands of reactions and hundreds of chemical species, among them many radicals that exist only for an instant of time, possibly generating very different results. It is also of fundamental importance to consider transport and thermodynamical properties for all those species. Additionally, the particularities of each kind of flame set also influence these characte-

istics. All that is necessary to comprehend pollutant formation, burning profiles, flame speed, temperatures, among other factors.

A global reaction for two given reactants can be described by the general formulation:



in which one molecule of A reacts with ν molecules of B , producing a generic final product P . In reality, there is a "black box" of intermediate reactions and products not considered in this formulation, for it is necessary to break many molecular bonds and form many others, in a process that involves many radicals. Instead, elementary reactions must be evaluated.

For example, in the process of the combustion of hydrogen in oxygen, one of the most extensively studied and better described, a global reaction can be presented as:



However, between reactants and products, the following elementary reactions are present:



among many others.

Chemical species that appear in those reactions, like H , OH , HO_2 , are the so-called radicals, or free radicals, the ones that present unpaired electrons, crucial for the formation of stable substances. The group of elementary reactions used to describe an overall reaction is known as a mechanism. Full scale kinetic schemes for fuels contain a number of those mechanisms, involved in the many phases of the combustion process.

In fact, the majority of the elementary reactions of interest in combustion are the bimolecular ones, in which two molecules collide, forming two other molecules. They can be described by the general formulation:



for A and B the two reactants and C and D the products. The reactions proceed at a rate directly proportional to the concentrations (in SI units, in $kmol/m_3$) of each reactant species, like in the equation 2.8:

$$\frac{d[A]}{dt} = -k_{bimolec}[A][B], \quad (2.8)$$

in which the rate coefficient, $k_{bimolec}$ (in SI units, $m^3/(kmol \cdot s)$), is a function of the temperature. Its value can be calculated through the collision theory. Physicochemical details are better explained in the works of Turns (2012) and Darabiha *et al.* (2006). In short, for a temperature range not too great, the value of the bimolecular rate coefficient can be expressed by the empirical Arrhenius equation (2.9):

$$k(T) = AT^b \exp\left(-\frac{E_A}{R_u T}\right), \quad (2.9)$$

where T is the temperature, while A , b and E_a are values taken from experimental data, from graphics that register the behavior of those reactions. E_A is the activation energy, a number that determines the minimum energy necessary for the reaction to happen, while R_u is the universal gas constant.

For unimolecular reactions, those with only one reactant, and termolecular reactions, the ones containing three reactants, the Arrhenius formulation is also valid. They are also considered elementary reactions, of great importance for combustion processes. In the first case, the one which describes typical dissociation reactions of burning, for example, the process is considered as a first-order one, at high pressures, as seen in the equation 2.10:

$$\frac{d[A]}{dt} = -k_{uni}[A], \quad (2.10)$$

and a second order one at low pressures, due to the collision that happens with another determinate species M , as seen in the equation 2.11:

$$\frac{d[A]}{dt} = -k[A][M], \quad (2.11)$$

also depending on the concentration of the species M . In the second case, reactions involving,

in general, a third body M , are of third order, presenting the formulation:

$$\frac{d[A]}{dt} = -k_{ter}[A][B][M], \quad (2.12)$$

in which the third body M acts in the energy transfers necessary to the formation of products. It is important to notice that this species M does not change its molecular structure in both kinds of reactions.

Values for the particle AT^b can be calculated by more complex formulations of the collision theory. Also, nowadays, more advanced theories for chemical kinetics have been capable of determining values for the activation energy based on the molecular structure and the process of breaking and forming bonds (Turns, 2012). However, for the practical applications of combustion, the Arrhenius formulation is sufficient. In general, the chemical kinetic schemes are presented in the form of tables, listing the elementary equations and their values for A , b and E_A for certain ranges of temperature. An example of part of a chemical kinetic scheme is the one below, in table 2.1.

Table. 2.1: Recommended rate coefficients for H_2 - O_2 reactions. Adapted from Turns (2012 apud. Warnatz, 1984)

Reaction	$A [(cm_3/gmol)^{n-1}/s]^a$	b	E_A (kJ/gmol)	Temperature Range (K)
$H + O_2 \rightarrow OH + O$	$1.2 \cdot 10^{17}$	-0.91	69.1	300-2,500
$OH + O \rightarrow O_2 + H$	$1.8 \cdot 10^{13}$	0	0	300-2,500
$O + H_2 \rightarrow OH + H$	$1.5 \cdot 10^7$	2.0	31.6	300-2,500
$OH + H_2 \rightarrow H_2O + H$	$1.5 \cdot 10^8$	1.6	13.8	300-2,500
$H + H_2O \rightarrow OH + H_2$	$4.6 \cdot 10^8$	1.6	77.7	300-2,500
$O + H_2O \rightarrow OH + OH$	$1.5 \cdot 10^{10}$	1.14	72.2	300-2,500
$H + H + M \rightarrow H_2 + M$				
$M = Ar(lowP)$	$6.4 \cdot 10^{17}$	-1.0	0	300-5,000
$M = H_2(lowP)$	$0.7 \cdot 10^{16}$	-0.6	0	100-5,000
$H_2 + M \rightarrow H + H + M$				
$M = Ar(lowP)$	$2.2 \cdot 10^{14}$	0	402	2,500-8,000
$M = H_2(lowP)$	$8.8 \cdot 10^{14}$	0	402	2,500-8,000
$H + OH + M \rightarrow H_2O + M$				
$M = H_2O(lowP)$	$1.4 \cdot 10^{23}$	-2.0	0	1,000-3,000
$H_2O + M \rightarrow H + OH + M$				
$M = H_2O(lowP)$	$1.6 \cdot 10^{17}$	0	478	2,000-5,000
$O + O + M \rightarrow O_2 + M$				
$M = Ar(lowP)$	$1.0 \cdot 10^{17}$	-1.0	0	300-5,000
$O_2 + M \rightarrow O + O + M$				
$M = Ar(lowP)$	$1.2 \cdot 10^{14}$	0	451	2,000-10,000

^afor n the reaction order

It is also important to notice that chemical kinetic schemes sometimes present quite different values for the same reactions. It happens due to the differences between the basic experiments in which they are based, or even differences in the way those numbers are taken from the graphics. When dealing with the manipulation of kinetic schemes, these factors must be taken into account.

2.2 One-Dimensional Laminar Premixed Flame

Laminar premixed flame is a flame set extensively used in residential, commercial and industrial applications. Basically, a laminar premixed flame is the one in which a mixture of fuel and oxidizer (in most cases, air) is injected in a certain control volume, is ignited and produces a laminar flame, in other words, in a flux in which fluid particles move themselves in parallel sheets (for the concept of laminar flow, see Fox *et al.* (2006)). Examples include ovens, heating appliances and Bunsen burners. Despite not being the process that happens in internal combustion engines - for those, turbulent flames are a more accurate set - many turbulent flame theories are based on features of the laminar flame structure, motivating its study. Additionally, laminar premixed flame studies are important for quantifying the flame speed, a value that dictates flame shape and important stability characteristics, such as blowoff and flashback. For basic science studies on the combustion of new fuels, these features are very important (Turns, 2012).

First of all, it is useful to define what a flame is. A flame is "a self-sustaining propagation of a localized combustion zone at subsonic velocities"(Turns, 2012). This definition implies some key features. A flame must be localized, that means it only occupies a certain portion of the combustible mixture at a certain moment in time. Secondly, it is subsonic, a discrete combustion wave that travels at a certain lower-than-the-sound velocity. This process is termed as a deflagration - which differs from that one called detonation, the propagation of the combustion wave at supersonic velocities. There is a completely different science behind this one, which will not be explained in the present work.

A common simplification very useful for basic combustion studies like the present one is to understand the laminar premixed flame as an one-dimensional entity. Despite not being a configuration very common in real applications of combustion, approximated one-dimensional flames can be recreated in laboratory for experimental studies, as further explained in the chapter, enabling the evaluation of laminar flame speed and temperature profiles for a certain case.

2.2.1 Main Characteristics

The temperature profile is sometimes considered its most important characteristic. Figure 2.1 illustrates a typical unidimensional profile, along with other important information.

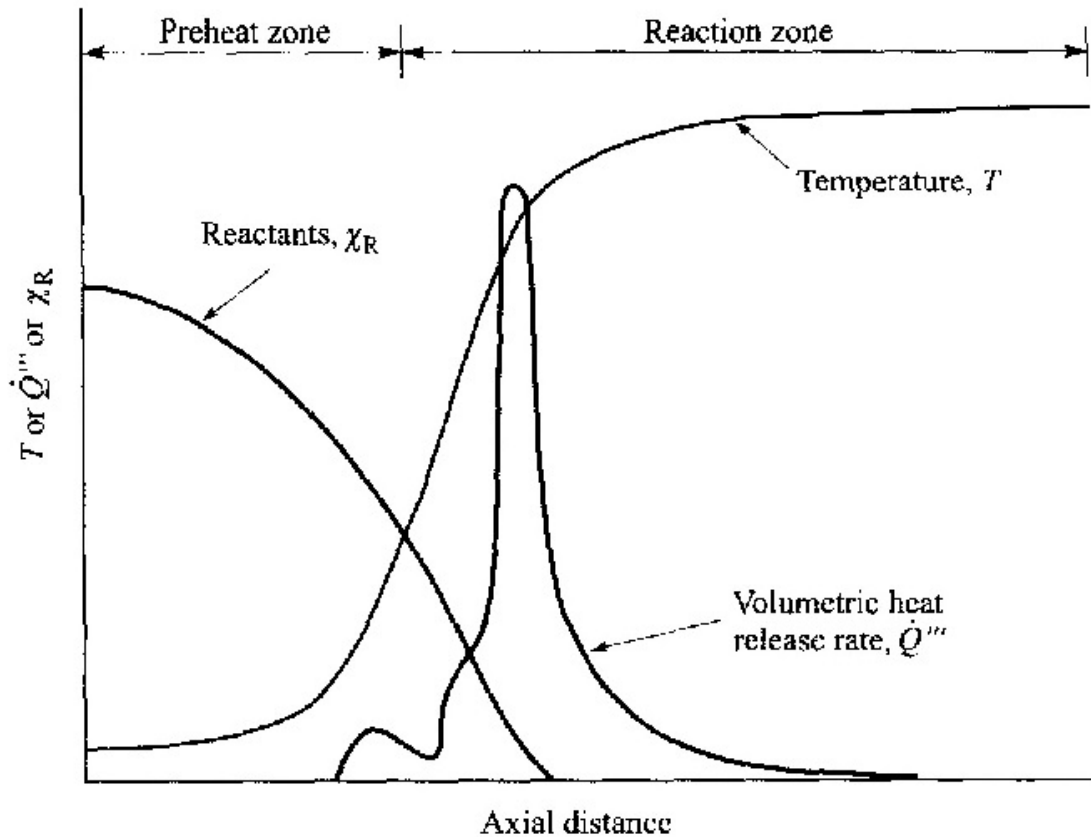


Figure. 2.1: Laminar flame structure. Source: Turns (2012).

This profile assumes that the flame is flat, behaving as a stationary entity, in which the flame location is kept by adjusting the velocity of the inlet premixed mixture flow to the value of the flame propagation velocity, in this case, called laminar flame speed, S_L . In this example, it is also assumed that the flame is one-dimensional, and that the mixture enters the flame in a direction normal to the flame sheet. The mass balance around the flame requires that

$$\rho_u S_L A = \rho_u v_u A = \rho_b v_b A, \quad (2.13)$$

in which the subscripts u and b refer to the unburned and burned gases, respectively. The laminar flame speed, S_L , can be described as the velocity at which an unstretched flame front moves, consuming reactants and producing burning gases. In typical hydrocarbon-air fla-

mes at atmospheric pressure, the density of the burned gases becomes about seven times lower than that of the unburned, greatly accelerating the flow.

As represented, it is common to divide the flame into two zones: the preheat zone, in which little energy is released, and the reaction zone, responsible for most of the energy released. In these conditions, it is also useful to divide the reaction zone into a thin region where very fast chemistry occur, followed by another, much wider region of slow chemistry. In the first region of the reacting zone, fuel molecules are broken, becoming many intermediate species, in predominantly bimolecular reactions. At atmospheric pressure, this zone is quite thin, in general measuring less than a millimeter, and due to that, temperature gradients and species concentration gradients are very large. These gradients are responsible for keeping the flame as a self-sustaining process, due to the heat and radical diffusion forced from the reaction zone to the preheat zone. In the following region, called secondary reaction zone, three-body radical recombination is predominant, in much slower reactions. In carbon-based fuels, it leads to the final burnout of CO , through the reaction:



Hydrocarbon flames, in most burning conditions, present visible radiation in the fast-reaction zone. It is the easiest way of locating the flame. It can appear in blue for the combustion of poor mixtures - the ones where there is more air than what is needed for the stoichiometric global reaction - due to the excitation of CH radicals, which become CH^* radicals. For rich mixtures, which have less air than in the stoichiometric proportion, the zone emits radiation in a blue-green color, due to excited C_2 radicals. Additionally, OH^* radicals also contribute to visible radiation and, to a lesser degree, chemiluminescence from the reaction:



for hv the light emission. For even richer flames, soot is formed, which emits blackbody continuum radiation in the range from bright yellow (almost white) to dull orange colors. Studies can be made to evaluate several flame characteristics through the analysis of the spontaneous light emissions of a burning fuel (Alviso *et al.*, 2015).

2.2.2 Flame Analysis

A flame is a complex phenomenon; however, it can be described using the conservation equations of the fluid mechanics and thermodynamics. A detailed description of the governing equations of reactant flows are presented in appendix A. In this chapter, the flame analysis is simplified to the one-dimensional case. Their solution cannot be made analytically, demanding numerical simulations, using computational tools, like the REGATH package. More information on them is described in the next chapter.

Considerations

Some assumptions are made in this analysis:

- Species behave as ideal gases.
- Steady state.
- One-dimensional flux.
- Pressure does not vary in the control volume.

Boundary conditions can also be set:

- Species concentrations up to the flame inlet and far from the flame zone are constant:

$$Y_k(x \rightarrow -\infty) = Y_{k,0}, \quad (2.16)$$

$$\frac{dY_k}{dx}(x \rightarrow \infty) = 0, \quad (2.17)$$

- Species concentrations at the flame inlet are known.
- Temperature up to the flame inlet and far from the flame zone are constant:

$$T(x \rightarrow -\infty) = T_0, \quad (2.18)$$

$$\frac{T}{dx}(x \rightarrow \inf) = 0, \quad (2.19)$$

- Temperature at the flame inlet and at a fixed location are known.

Those assumptions greatly simplify this analysis, making computer calculations much faster, even not requiring explicit momentum conservation equations. The formulation, considering those conditions, is explained below.

Continuity

$$\frac{d\dot{m}''}{dx} = 0. \quad (2.20)$$

Species Conservation

For a steady one-dimensional flow, in which \dot{m}_i''' can be replaced by $\dot{\omega}_i W_i$ in the general equation A.11:

$$\frac{d}{dx}(\rho v_x Y_i) + \frac{d}{dx}(\rho Y_i v_{i,diff}) = \dot{\omega}_i W_i, \text{ for } i = 1, 2, \dots, N, \quad (2.21)$$

where $\dot{\omega}_i$ is the molar production rate of species i , from the equation 2.8.

Energy Conservation

Starting with equation A.28, a general form for N species, in which a mixture $c_p = \sum Y_i c_{p,i}$ in any one-dimensional laminar flame set can be set as:

$$\dot{m}'' c_p \frac{dT}{dx} + \frac{d}{dx} \left(-k \frac{dT}{dx} \right) + \sum_{i=1}^N \rho Y_i v_{i, diff} c_{p, i} \frac{dT}{dx} = - \sum_{i=1}^N h_i \dot{m}_i''' \quad (2.22)$$

By replacing \dot{m}_i''' by $\dot{\omega}_i W_i$, equation 2.22 becomes:

$$\dot{m}'' c_p \frac{dT}{dx} + \frac{d}{dx} \left(-k \frac{dT}{dx} \right) + \sum_{i=1}^N \rho Y_i v_{i, diff} c_{p, i} \frac{dT}{dx} = - \sum_{i=1}^N h_i \dot{\omega}_i W_i \quad (2.23)$$

Other auxiliary relations are also necessary to the full calculations:

- Ideal-gas equation of state.
- Constitutive relations for diffusion velocities.
- Temperature-dependent species properties: $h_i(T)$, $c_{p, i}(T)$, $k_i(T)$ and $D_{ij}(T)$
- Mixture property relations to calculate $W_{mixture}$, k , D_{ij} and D_i^T from data from individual species.
- A detailed chemical kinetic mechanism.
- Conversion relations for molar and mass fractions.

These relations are available in the next section of this chapter, based on the works of Darabiha *et al.* (2006) and Turns (2012).

2.3 Auxiliary Properties

For the analysis of combustion flows, there are two kinds of properties that complement the equations: the thermodynamic properties and the transport properties. The parameters defined in these categories are very important for the formulations of the combustion phenomenon, such as the diffusivity coefficient and the specific heat. The methods for calculating them computationally are described in this section.

2.3.1 Thermodynamic Properties

The main thermodynamic properties used in applications involving heat transfer, energy conservation, among others, are the specific heat, c_p , the specific enthalpy, h , and the specific entropy, s . Their values are different for each species and temperature, and methods are being developed for their calculations in numerical combustion applications.

One of those methods is the one described by Darabiha *et al.* (2006), which uses 14 coefficients to define fourth-order polynomial equations, which approximate those values for a certain range of temperatures. Data for them comes from experiments that study their characteristics for each temperature.

It is assumed that the species involved in the calculations behave as perfect gases; therefore, they follow the equation:

$$\rho = \frac{pW}{R_u T}, \quad (2.24)$$

for p the pressure, W the molar mass, R_u the universal gas constant and T the absolute temperature. In this sense, the specific enthalpy of a certain mixture can be calculated as:

$$h = \sum_{k=1}^K Y_k h_k, \quad (2.25)$$

for species $k = 1, \dots, K$. Y_k is the concentration for the species k in the mixture. Defining c_{pk} as:

$$c_{pk} = \left(\frac{dh_k}{dT} \right)_p \quad (2.26)$$

the enthalpy of the species k can be presented as:

$$h_k = h_k(T_0) + \int_{T_0}^T c_{pk}(T') dT', \quad (2.27)$$

where $h_k(T_0)$ is the standard formation enthalpy at the reference temperature T_0 . For the mixture, its c_p can be defined by:

$$c_p = \sum_{k=1}^K Y_k c_{pk}, \quad (2.28)$$

so that the the specific enthalpy of the mixture can be described as:

$$h = \sum_{k=1}^K h_k(T_0)Y_k + \sum_{k=1}^K Y_k \int_{T_0}^T c_{pk}(T')dT'. \quad (2.29)$$

In an analogous way, the entropy of the mixture can be expressed by:

$$s = \sum_{k=1}^K Y_k s_k, \quad (2.30)$$

being s_k the entropy for a species k , which can be given by the equation:

$$s_k = s_k(T_0, p_0) + \int_{T_0}^T \frac{c_{pk}(T')}{T'}dT' - \frac{R}{W_k} \log \frac{p_k}{p_0}, \quad (2.31)$$

for $s_k(T_0, p_0)$ the standard formation entropy at the reference temperature T_0 and pressure p_0 , while p_k is the partial pressure of the species k . In particular, by taking $s_k^0 = s_k^0(T)$, the entropy of the k th species at atmospheric pressure $p_k = p_0 = p_{atm}$, the following equation is formed:

$$s_k^0 = s_k(T_0, p_0) + \int_{T_0}^T \frac{c_{pk}(T')}{T'}dT'. \quad (2.32)$$

Finally, the thermodynamic properties can be deducted from the correspondent molar properties, in the relations:

$$c_{pk} = \frac{C_{pk}}{W_k}, \quad h_k = \frac{H_k}{W_k}, \quad s_k^0 = \frac{S_k^0}{W_k}. \quad (2.33)$$

Those molar properties are the ones that can be calculated through the approximation polynomials:

$$\frac{C_{pk}}{R_u} = \begin{cases} a_{1k} + a_{2k}T + a_{3k}T^2 + a_{4k}T^3 + a_{5k}T^4 \\ \text{if } T_{inf} \leq T \leq T_{med} \\ a_{8k} + a_{9k}T + a_{10k}T^2 + a_{11k}T^3 + a_{12k}T^4 \\ \text{if } T_{med} \leq T \leq T_{sup} \end{cases} \quad (2.34)$$

$$\frac{H_k}{R_u} = \begin{cases} a_{1k} + \frac{a_{2k}}{2}T + \frac{a_{3k}}{3}T^2 + \frac{a_{4k}}{4}T^3 + \frac{a_{5k}}{5}T^4 + \frac{a_{6k}}{T} \\ \text{if } T_{inf} \leq T \leq T_{med} \\ a_{8k} + \frac{a_{9k}}{2}T + \frac{a_{10k}}{3}T^2 + \frac{a_{11k}}{4}T^3 + \frac{a_{12k}}{5}T^4 + \frac{a_{13k}}{T} \\ \text{if } T_{med} \leq T \leq T_{sup} \end{cases} \quad (2.35)$$

$$\frac{S_k}{R_u} = \begin{cases} a_{1k} \log T + a_{2k}T + \frac{a_{3k}}{2}T^2 + \frac{a_{4k}}{3}T^3 + \frac{a_{5k}}{4}T^4 + a_{7k} \\ \text{if } T_{inf} \leq T \leq T_{med} \\ a_{8k} \log T + a_{9k}T + \frac{a_{10k}}{2}T^2 + \frac{a_{11k}}{3}T^3 + \frac{a_{12k}}{4}T^4 + a_{14k} \\ \text{if } T_{med} \leq T \leq T_{sup} \end{cases} \quad (2.36)$$

considering $[T_{inf}, T_{med}]$ and $[T_{med}, T_{sup}]$ approximation ranges related to inferior, medium and superior temperatures, experimentally determined, and constants a_{1k}, \dots, a_{14k} empirical. a_{6k} and a_{13k} are the reference enthalpies linked to the formation enthalpies at $0K$ and a_{7k} and a_{14k} are the reference entropies linked to the formation entropies at $0K$.

Chemical kinetic schemes generally include a file for thermodynamic properties, which contains a list of the 14 coefficients and the temperature ranges for each of the involved species.

2.3.2 Transport Properties

As seen in the previous section (1.2), many of the conservation equations used in the combustion science depend on some transport properties, such as the binary diffusivity coefficient, viscosity and thermal conductivity. These properties depend on the interaction between the species in a combustion environment, temperature and pressure. Therefore, for computer simulations, it is necessary to use certain formulation capable of finding those parameters based on fixed variables, related to each species involved in the combustion, in a similar way to what happened for the thermodynamic properties.

Viscosity

Viscosity is a transport property that can be expressed based on state variables. According to Darabiha *et al.* (2006) and Kee *et al.* (2000), values for this property can be calculated by the equation:

$$\mu_k = \frac{5}{15} \frac{\sqrt{\pi W_k k_B T}}{\pi \sigma_k^2 \Omega^{(2,2)*}}, \quad (2.37)$$

where T is the temperature, σ_k is the collision diameter, k_B the Boltzmann constant, W_k the molecular mass and $\Omega^{(2,2)*}$ one type of collision integral, based on Stockmayer potentials. This last value depends on the reduced temperature, given by the expression:

$$T^* = k_B T / \varepsilon_k \quad (2.38)$$

and also the reduced dipole moment given by:

$$\delta_k^* = \frac{1}{2} \frac{\beta_k^2}{\varepsilon_k \sigma_k^3}, \quad (2.39)$$

where ε_k is the Lennard-Jones potential well depth and β_k the dipole moment. The collision integrals were tabulated by Monchick and Mason (1962), available in the literature.

Binary Diffusion Coefficient

This property is here described based on the works of Kee *et al.* (2000) and Darabiha *et al.* (2006). The binary diffusion coefficients are given in terms of pressure and temperature as:

$$D_{jk} = \frac{3}{16} \frac{\sqrt{2\pi k_b^3 T^3 / W_{jk}}}{P \pi \sigma_{jk}^2 \Omega^{(1,1)*}} \quad (2.40)$$

for W_{jk} the reduced molecular mass for the (j, k) species pair:

$$W_{jk} = \frac{W_j W_k}{W_j + W_k} \quad (2.41)$$

where W_j and W_k are their molecular masses. σ_{jk} is the reduced collision diameter. The collision integral $\Omega^{(1,1)*}$, also based on Stockmayer potentials, depends on the reduced temperature T_{jk}^* , which in turn is dependent on the species dipole moment, β_k , and polarizabilities, α_k . Reduced quantities, used in the calculations, depend on whether the collision partners are polar or nonpolar. If they are both polar or nonpolar, the following expressions apply:

$$\frac{\varepsilon_{jk}}{k_B} = \sqrt{\left(\frac{\varepsilon_j}{k_B}\right)\left(\frac{\varepsilon_k}{k_B}\right)} \quad (2.42)$$

$$\sigma_{jk} = \frac{1}{2}(\sigma_j + \sigma_k) \quad (2.43)$$

$$\beta_{jk}^2 = \beta_j \beta_k, \quad (2.44)$$

while for an interaction between a nonpolar molecule and a polar molecule:

$$\frac{\varepsilon_{np}}{k_B} = \xi^2 \sqrt{\left(\frac{\varepsilon_n}{k_B}\right)\left(\frac{\varepsilon_p}{k_B}\right)} \quad (2.45)$$

$$\sigma_{np} = \frac{1}{2}(\sigma_n + \sigma_p) \xi \left(-\frac{1}{6} \right) \quad (2.46)$$

$$\beta_{np}^2 = 0, \quad (2.47)$$

where:

$$\xi = 1 + \frac{1}{4} \alpha_n^* \beta_p^* \sqrt{\frac{\varepsilon_p}{\varepsilon_n}}. \quad (2.48)$$

In the expressions above, α_n^* is the reduced polarizability for the nonpolar molecule and β_p^* the reduced dipole moment for the polar molecule. They are given by:

$$\alpha_n^* = \frac{\alpha_n}{\sigma_n^3} \quad (2.49)$$

$$\beta_p^* = \frac{\beta_p n}{\sqrt{\varepsilon_p \sigma_p n^3}}, \quad (2.50)$$

and, for the temperature:

$$T_{jk}^* = k_B T / \varepsilon_{jk}. \quad (2.51)$$

Finally, for the reduced dipole moment:

$$\delta_{jk}^* = \frac{1}{2} \beta j k^{*2}, \quad (2.52)$$

Thermal Conductivity

Another important value, the thermal conductivity is composed of translational, rotational and vibrational molecular contributions, as stated in:

$$\lambda_k = \frac{\mu_k}{W_k} (f_{trans} C_{v,trans} + f_{rot} C_{v,rot} + f_{vib} C_{v,vib}), \quad (2.53)$$

where:

$$f_{trans} = \frac{5}{2} \left(1 - \frac{2}{\pi} \frac{C_{v,rot}}{C_{v,trans}} \frac{A}{B} \right) \quad (2.54)$$

$$f_{rot} = \frac{\rho D_{kk}}{\mu_k} \left(1 + \frac{2}{\pi} \frac{A}{B} \right) \quad (2.55)$$

$$f_{rot} = \frac{\rho D_{kk}}{\mu_k} \quad (2.56)$$

and:

$$A = \frac{5}{2} - \frac{\rho D_{kk}}{\mu_k} \quad (2.57)$$

$$B = Z_{rot} + \frac{2}{\pi} \left(\frac{5}{3} \frac{C_{v,rot}}{R} + \frac{\rho D_{kk}}{\mu_k} \right). \quad (2.58)$$

Molar heat capacities, stated by $C_{vk} = C_{pk} - R_u$, can be defined for the translational case as:

$$C_{v,trans} = \frac{3}{2} R_u \quad (2.59)$$

for any type of molecule. However, for a linear molecule:

$$C_{v,rot} = 1 \quad (2.60)$$

$$C_{v,vib} = C_v - \frac{5}{2}R_u. \quad (2.61)$$

In the case of a nonlinear molecule:

$$C_{v,rot} = \frac{3}{2}R_u \quad (2.62)$$

$$C_{v,vib} = C_v - 3R_u. \quad (2.63)$$

Finally, for molecules composed by a single atom:

$$C_{v,rot} = C_{v,vib} = 0. \quad (2.64)$$

In order to define the parameters, Z_{rot} and D_{kk} have yet to be described. The first one comes from the formula:

$$Z_{rot}(T) = Z_{rot}(298K) \frac{F(298K)}{F(T)}, \quad (2.65)$$

where:

$$F(T) = 1 + \frac{\pi^{3/2}}{2} \left(\frac{\varepsilon/k_b}{T} \right)^{1/2} + \left(\frac{\pi^2}{4} + 2 \right) \left(\frac{\varepsilon/k_b}{T} \right) + \pi^{3/2} \left(\frac{\varepsilon/k_b}{T} \right)^{3/2}, \quad (2.66)$$

while the second comes from the self-diffusion equation:

$$D_{kk} = \frac{3}{16} \frac{\sqrt{2\pi k_b^3 T^3 / W_k}}{P \pi \sigma_k^2 \Omega^{(1,1)*}}. \quad (2.67)$$

Density, however, comes from the equation of state for a perfect gas:

$$\rho = \frac{PW_k}{R_u T}. \quad (2.68)$$

2.4 Common Laminar Premixed Laboratory Flames

One of the most common types of burner for laminar premixed combustion tests is the Bunsen burner, as seen in figure 2.2. It consists on a tube device in which a jet of fuel is injected, and variable area ports through which air enters, forced by the fuel jet, mixing both components. Typically, a Bunsen burner is a dual flame, containing a primary rich premixed flame surrounded by a diffusion flame, produced by the contact between carbon monoxide and hydrogen products and the outer air. For this set, a stable, stationary flame must be formed by equaling the speed of the normal component of the unburned gas velocity. Therefore, as seen in figure 2.2, laminar flame speed can be calculated by:

$$S_L = v_u \sin \alpha, \quad (2.69)$$

being v_u the speed of the unburned gases and α the inner cone angle.

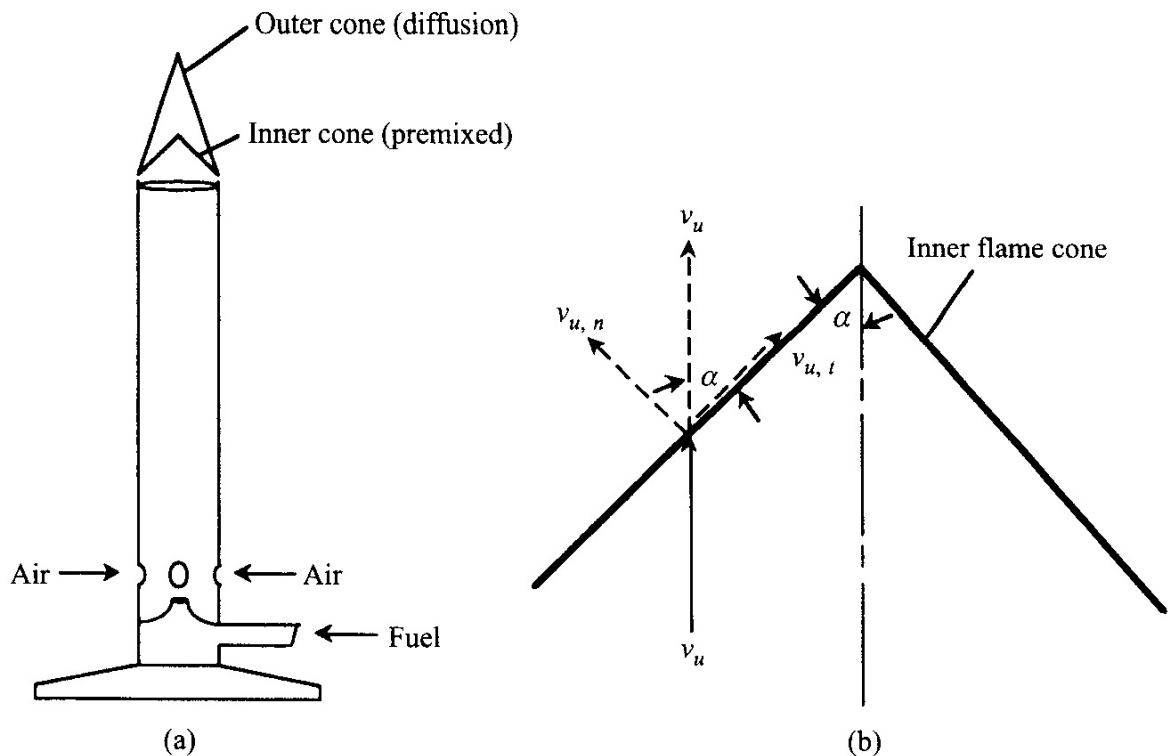


Figure. 2.2: (a) Bunsen-burner schematic. (b) Laminar flame speed equaling the normal component of the unburned gas velocity, $v_{u,n}$. Source: Turns (2012).

Other way of studying premixed laminar flames in a laboratory is in the one-dimensional flat-flame configuration. In order to run experiments that approximate to this ideal

condition, an adiabatic burner can be used, in which a bundle of small tubes conduct the fuel-air mixture in a laminar flux, being able to produce a stable flat flame in a range of conditions. On the other hand, non-adiabatic burners can also be used, extracting heat from the flame and decreasing its speed, allowing stabilization for a wide range of conditions. Both can be seen in figure 2.3

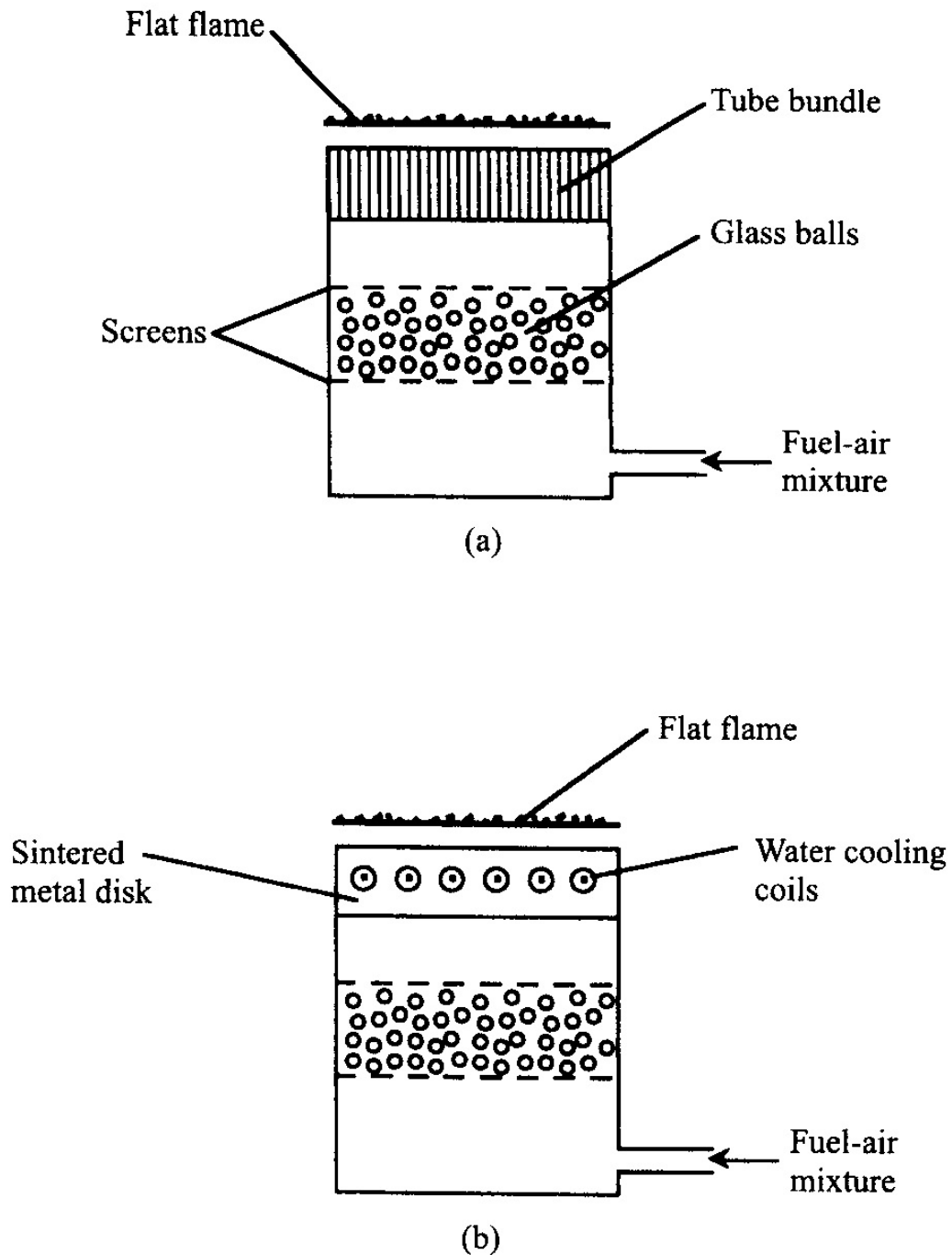


Figure. 2.3: (a) Adiabatic flat-flame burner. (b) Non-adiabatic flat-flame burner. Source: Turns (2012).

Finally, another common experimental set used in laminar premixed flame evaluation is the constant-volume spherical bomb (also called constant-volume vessel or constant volume reactor)(Coelho and Costa, 2012). In this set, fuel and air or other oxidant are mixed inside a spherical closed chamber, then ignited. A spherically-shaped flame is then formed, and due to the expansion of the burned gases, the pressure inside the chamber increases continually. This variation, added to the flame front position as a function of time, is considered in the definition of the laminar flame speed, which follow the relation:

$$S_L = \left(1 - \frac{R^3 - r^3}{3p\gamma r^2} \frac{dp}{dr}\right) \frac{dr}{dt}, \quad (2.70)$$

for R the bomb radius, p and r are the pressure and flame radius at a certain moment in time (t). γ is the relation between the constant pressure and constant volume specific heat capacities of the unburnt mixture, $\gamma = c_p/c_v$. Figure 2.4 represents this device.

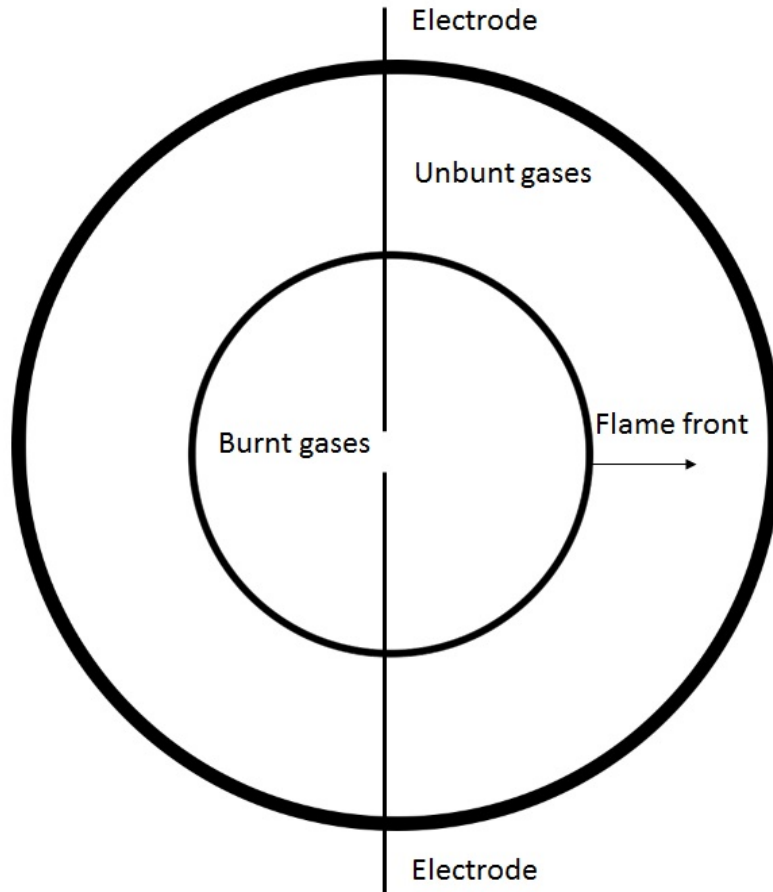


Figure. 2.4: Constant-volume spherical bomb

2.5 State-of-the-Art

2.5.1 Kinetic Schemes

Kinetic schemes, as previously explained, detail the reactions involved in the combustion of a certain fuel. Those models are very useful for a range of computer simulations involving not only basic combustion studies but also engine simulations. Studies for new fuels in laminar conditions, as seen in the works of Alviso *et al.* (2015) for biodiesel, Man *et al.* (2014) for propanol, and many others, develop and use those schemes. On the other hand, Large Eddy Simulation (LES) (Darabiha *et al.*, 2006), a technique that simulates turbulent burning in several applications, relies on chemical mechanisms for its analysis.

The development of kinetic schemes involves series of studies, many times run by different teams in different parts of the globe. Many times, these groups base their studies in experiments ran by the same people, in schemes developed for fuels of less complex molecular composition that might be not the same, generating variations. Therefore, kinetic schemes available in the literature present some differences related to the number of reactions, their types and their rates, the number and type of evaluated species and also their thermodynamic and transport properties. All that influences the behavior of the kinetic scheme, the range of pressures, temperatures and primary species to which they are valid.

The main purpose of this work was to develop methods of evaluating the combustion of blends between n-butanol and ethanol. In this sense, it is important to search in the literature for state-of-the-art information in kinetic schemes for both fuels. This section presents information on them.

N-Butanol

N-butanol, as previously cited, is one of the most promising substances proposed as biofuels for commercial applications. Due to that, many studies have been done in recent years, such as the ones from Dagaut *et al.* (2009) and Jin *et al.* (2014), and many others are being developed. However, it is a difficult task to find chemical schemes available in full in the

literature. Additionally, depending on the type and version of the software package used, some files cannot be run in REGATH simulations, and its models could not be tested.

For the present work, two kinetic schemes from the same first author, but different groups, were taken for comparison. The oldest one, presented in the article of Sarathy *et al.* (2009), comprises 118 species and 878 reactions for the combustion of n-butanol; tests were made in a jet stirred reactor (JSR) and in a counterflow diffusion burner for species mass fractions, and in a spherical flame propagation set for laminar flame speed. The second one, that of the work of Sarathy *et al.* (2012), is a detailed model for the four butanol isomers, and contains 426 species and 2335 reactions, including a mechanism for the combustion of ethanol; its validation was done by comparing simulated values with those in the literature, for both flame speed and species concentrations.

Ethanol

Ethanol is one of the best studied biofuels. Kinetic schemes for the combustion of pure ethanol and its blends with gasoline surrogates (Rau *et al.*, 2015) are widely available. Among them, some cannot be run in REGATH (Liu *et al.*, 2011), or its codings were not available in the literature.

Experiments and numerical simulation made by Leplat *et al.* (2011) are very important for the evaluation of ethanol combustion characteristics. Chemical species' mole fractions were evaluated at a flat-flame burner and a jet-stirred reactor (JSR), while the developed mechanism, containing 252 reactions (not counting duplicates) and 60 species. Perhaps due to differences between the software used in its development and the one used in the present work, this scheme could not be tested.

For the present work, ethanol schemes from Marinov (1999) and Konnov *et al.* (2011) were chosen. The first article presents a simple, strongly consolidated model for ethanol, containing 57 species and 383 reactions; this model was validated by comparison with previous works in a constant volume bomb and in a counterflow twin-flame burner for laminar flame speed, and in a jet-stirred and a turbulent flow reactors for species profiles. The second one, a more recent scheme, contains 129 species and 1231 reactions, and was tested experimentally in a flat-flame adiabatic burner, for both temperature profiles and laminar flame speed.

2.5.2 Experimental Data

Experimental data was taken exclusively from the literature, due to the lack of experimental resources available for the research. In order to maintain data agreement, it was decided that the values for temperature and pressure should not be too different, in order to avoid huge disparities between flame speeds; in fact, for this reason, most of the chosen data was taken at the same temperature and pressure, limiting the number of studies reviewed in this work.

N-Butanol

The experiments that provide data for n-butanol are those from the works of Sarathy *et al.* (2009), Zhang *et al.* (2013) and Liu *et al.* (2011).

The one from Sarathy *et al.* (2009), as previously cited, was run in a spherical flame propagation set for laminar flame speed, in a combustion bomb, detailed in the article. The pressure and temperature conditions were selected to optimize the saturated vapor pressure of butanol. Fuel-air equivalence ratios are within a range between 0.8 and 1.2. The measurements have an estimated uncertainty of ± 2 cm/s. For this work, the results for a pressure of 0.89 atm and temperature of 350 K were chosen.

The work of Liu *et al.* (2011) presents a experiment done in a heated, dual-chambered combustion vessel, which generates outwardly propagating spherical flames, described in the article. It also provides a kinetic scheme, unable to run in REGATH due to differences in file coding. Initial temperature was set at 353 K, while pressures were set at 1 atm and 2 atm. Fuel-air equivalence ratios are within a range between 0.7 and 1.6. The measurements have an estimated uncertainty of ± 2 cm/s and the equivalence ratios have an uncertainty of $\pm 2\%$. The results for 1 atm were chosen for this work.

Finally, the work of Zhang *et al.* (2013) presents data obtained in a combustion bomb, in a spherically expanding flame set, at temperatures ranging from 353 K to 433 K. Pressure was kept at 1 atm. Fuel-air equivalence ratios are within a range between 0.8 and 1.5. The measurements have an estimated uncertainty of ± 1.4 cm/s. For the present work, data for the temperature of 353 K was chosen for comparison.

Ethanol

For ethanol, the works of van Lipzig *et al.* (2011) and Konnov *et al.* (2011) provide data for laminar flame speed.

As cited, the work of Konnov *et al.* (2011) tests the burning of ethanol in an adiabatic flat-flame burner, using the Heat Flux method for the measurements. Initial temperatures were set from 298 K to 358 K, at atmospheric pressure (1 atm). Fuel-air equivalence ratios are within a range between 0.65 and 1.25, due to flammability limits in this experimental setup. The measurements have an estimated uncertainty of ± 1 cm/s. The present work uses data from the experiment at 298 K for comparison.

The work of van Lipzig *et al.* (2011) presents an experiment made on a flat-flame burner, equipped with an evaporator for liquid fuels. It uses the Heat Flux method for the evaluation of the flame. Temperatures were set to 298 K and 338 K, while the pressure was kept at 1 atm. Fuel-air equivalence ratios are within a range between 0.6 and 1.2, due to flammability limits in this experimental setup. The measurements have an estimated uncertainty of ± 1 cm/s. This research tries to construct and certify an experimental rig very similar to that of Konnov *et al.* (2011). Again, the present work uses data from the experiment at 298 K for comparison.

N-Butanol and Ethanol Studies

Studies on blends between ethanol and n-butanol were not found in the literature. However, the work of Broustail *et al.* (2011) provided an important study on laminar flame speed for both fuels in their pure form and also blended with iso-octane. All substances were tested in a constant-volume vessel, using the spherical expanding flame methodology. The tested initial pressure was 1 bar, and the initial temperature was kept at 393 K. Fuel-air equivalence ratios ranged from 0.8 to 1.4. The perceived uncertainty was up to ± 3 cm/s, however, the calculated values were not made available.

The work of Broustail *et al.* (2011) is considered paramount for this study. Despite not being a study on blends between both alcohols, the fact that both were tested at the same conditions, in the same equipments, makes the results, in theory, very credible for a comparison

between the combustion characteristics of both fuels. The graphic presented in figure 2.5 shows their behavior in that flame set.

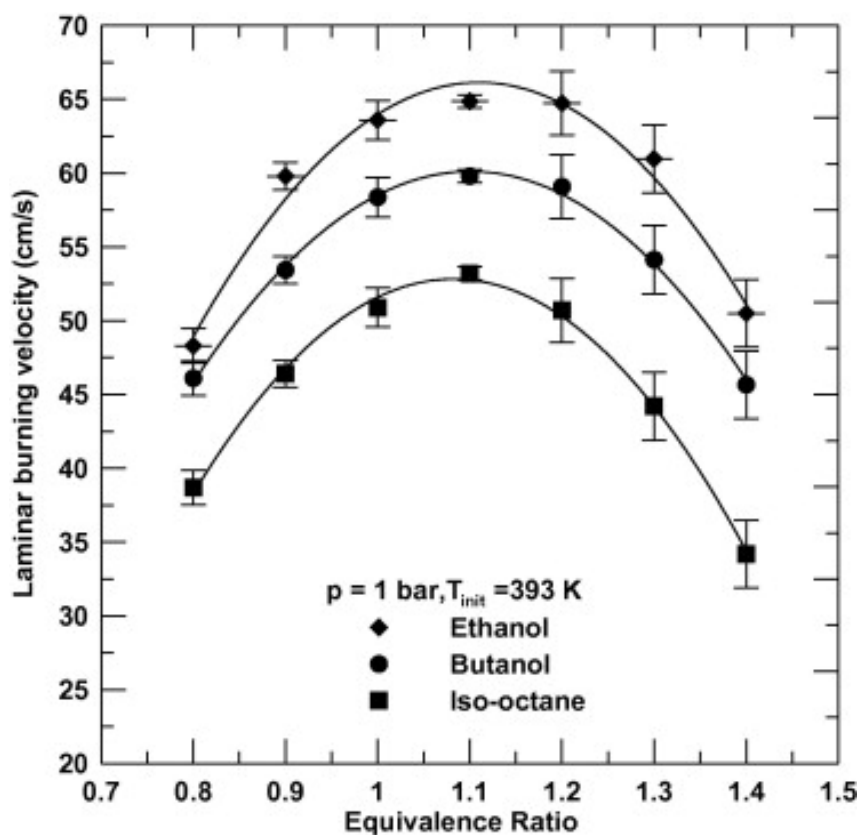


Figure. 2.5: Laminar flame speed for ethanol, n-butanol and iso-octane. Adapted from Broustail *et al.* (2011).

As seen above, at atmospheric conditions, ethanol presents higher flame speeds when compared to n-butanol (and also iso-octane). This is a characteristic further evaluated and discussed, for the validation of the studied kinetic schemes.

2.6 Summary of the Works on Ethanol and N-Butanol

The following table (2.2) summarizes the experimental and numerical works evaluated for both fuels. Details on the modeling and validation of kinetic schemes and experimental conditions are presented in the original texts, available in the most common Internet-based scientific databases.

Table. 2.2: Comparison between laminar flame speed works for n-butanol and ethanol combustion

Fuel	Reference	Number of species and reactions	Experimental data constraints	Experimental set/ Validation method
N-Butanol	Sarathy <i>et al.</i> (2009)	118 species and 878 reactions	$p_0 = 0.89 atm$ $T_0 = 350 K$ $\phi = 0.8 - 1.2$ $e = \pm 2 cm/s$	JSR (jet stirred reactor) and counterflow diffusion burner for species mass fractions; spherical flame propagation set for laminar flame speed, in a combustion bomb.
N-Butanol	Liu <i>et al.</i> (2011)	117 species and 884 reactions	$p_0 = 1 atm, 2 atm$ $T_0 = 353 K$ $\phi = 0.7 - 1.6$ $e = \pm 2 cm/s, \delta\phi = \pm 2\%$	Laminar flame speed evaluated in dual-chambered combustion vessel, set for outwardly propagating spherical flames.
N-Butanol and Ethanol	Broustail <i>et al.</i> (2011)	No numerical simulation	$p_0 = 1 bar$ $T_0 = 393 K$ $\phi = 0.8 - 1.4$ $e = \pm 3 cm/s$	Laminar flame speed evaluated in constant-volume vessel, for both n-butanol and ethanol.

N-Butanol and Ethanol	Sarathy <i>et al.</i> (2012)	426 species and 2335 reactions	No experiment	Comparison between simulated data and various experiments from the literature, for both laminar flame speed and species concentrations.
N-Butanol	Zhang <i>et al.</i> (2013)	No numerical simulation	$p_0 = 1atm$ $T_0 = 353K, 433K$ $\phi = 0.8 - 1.5$ $e = \pm 1.4cm/s$	Laminar flame speed evaluated in a combus- tion bomb, in a spherically expanding flame set.
Ethanol	Marinov (1999)	57 species and 383 reac- tions	No experiment	Comparison between simulated data and various experiments from the literature, for both laminar flame speed and species concentrations.
Ethanol	Konnov <i>et al.</i> (2011)	129 species and 1231 reactions	$p_0 = 1atm$ $T_0 = 298K - 358K$ $\phi = 0.65 - 1.25$ $e = \pm 1cm/s$	Temperature profiles and laminar flame speed evaluated in a flat-flame burner, using the Heat Flux method.
Ethanol	Leplat <i>et al.</i> (2011)	60 species and 252 reac- tions	No experiment for flame speed	Species profiles evaluated in a flat-flame bur- ner and a JSR.

Ethanol	van Lipzig <i>et al.</i> (2011)	No numerical simulation	$p_0 = 1atm$ $T_0 = 298K, 338K$ $\phi = 0.6 - 1.2$ $e = \pm 1cm/s$	Laminar flame speed evaluated in a flat-flame burner, using the Heat Flux method.
---------	---------------------------------	-------------------------	---	---

3 METHODOLOGY

The present work involved the following parts: (1) comparison between ethanol and n-butanol kinetic schemes and experimental data related to them; (2) rising of curves for simulated mixtures between both fuels, in many proportions, based on the model from Sarathy *et al.* (2012); (3) development of a combined scheme for ethanol and n-butanol; (4) raising of new curves for mixtures, based on the new model. All the simulations were made using the package REGATH, as described in the following sections.

3.1 Numerical Simulation Parameters

For the simulations ran in this research, some parameters were kept in order to obtain information valid for the purposes of the work.

3.1.1 Target Data

The present work intended to compare chemical kinetic schemes and experimental data for both n-butanol and ethanol, and further developing a new scheme for blends between them. For that reason, the chosen characteristics to be compared were the laminar flame speed, the temperature profiles and the species mass concentration.

The laminar flame speed was compared in all the phases of the research, being one of the simplest to determine and most important characteristics of the burning process. It was taken as the main value to determine the quality of the kinetic scheme, indicating whether or not it was valid for a certain fuel. This data was evaluated for a range of fuel-air equivalence ratios, and for every kinetic scheme compared in this study.

The temperature profile is a very important feature of the flame. It was evaluated numerically for the blends and the pure substances in the new scheme, however, this data was not validated, considering it was not available for comparison in the evaluated conditions.

The species mass concentration for C_2H_5OH (ethanol), C_4H_9OH (n-butanol), O_2 ,

CO_2 , H_2O and CO were also evaluated in the simulations for the pure substances in the new scheme, however, due to the lack of available experimental data in the simulated conditions, validation for this set could not be done.

3.1.2 Flame Set

The chosen flame set was that of one-dimensional premixed laminar flame. As previously explained in chapter 2, it is one of the simplest flame configurations, faster to run computationally and to be studied in experiments. Premixed laminar flame sets are some of the most widely used sets for defining laminar flame speed and, despite not being the configuration present in internal combustion engines, theories behind turbulent combustion are based on laminar premixed flames; additionally, chemical schemes evaluated and validated in laminar conditions can be used in turbulent conditions, motivating previous work in that set (Turns, 2012).

It is also important to notice that all simulations were made for combustion on air, which was defined as containing 21% in volume of oxygen (O_2) and 79% of nitrogen (N_2).

3.1.3 Initial Temperature and Pressure

The initial temperature and pressure set for the simulations depend on the parameters used in the experiments that provide data for comparison.

For ethanol, considering the chosen experiments of Konnov *et al.* (2011) and van Lipzig *et al.* (2011), which initial temperature was 298K (room temperature) and pressure was 1 atm, all simulations for this fuel were set for the same parameters.

For n-butanol, considering the chosen experiment of Sarathy *et al.* (2009) being run at 350K and the ones from Liu *et al.* (2011) and Zhang *et al.* (2013) at 353K, the temperature from the latter two was chosen for the comparison between models and experiments. The pressure for the experiment of Sarathy *et al.* (2009) was of 0.89 atm, and for the others, 1 atm; the second value was the one reproduced in the simulations. The differences produced by the different pressures and temperatures were considered minimal, due to the low numerical distance between the values and due to the compensating effects of lower temperature and pressure, as

stated in chapter 8 of Turns (2012).

For blends, the initial temperature of 298K was the chosen one, for being simple to be reproduced in an experimental environment, as well as the pressure of 1 atm. Most experimental sets can run in those conditions.

3.1.4 Fuel-Air Equivalence Ratios

Fuel-air equivalence ratio is the relation between the stoichiometric air-fuel mass ratio and the air-fuel ratio on the mixture, given by the equation:

$$\phi = \frac{(A/F)_{stoic}}{(A/F)} = \frac{(m_{fuel}/m_{air})}{(m_{fuel}/m_{air})_{stoic}}, \quad (3.1)$$

for m_{fuel} the mass (or the mass fraction) of the fuel, m_{air} the one of the air and the subscript *stoic* relative to the stoichiometric values. In this research, ϕ values were set close to the stoichiometric mixture, simulating the conditions of most experiments at atmospheric pressure and spark-ignited internal combustion engines. In the comparison between chemical schemes from the literature, values range from 0.5 to 1.5 for n-butanol and from 0.5 to 1.7 for ethanol, with a 0.1 step between measurements. Some kinetic schemes could not converge up to those limits, due to possible flammability limits present in the schemes. In turn, species mass concentrations and temperature profiles were evaluated at

3.1.5 REGATH

REGATH is the name of a package of softwares written in FORTRAN capable of simulating laminar combustion in a series of flame configurations. It was developed in France by the laboratory EM2C, a CNRS fellow, linked to the CentraleSupélec (previously Ecole Centrale Paris), and courteously provided for the present work. Among others, laminar premixed flames, counterflow diffusion flames and double premixed flames for liquid and gaseous fuels can be evaluated through this tool, since it reads chemical kinetic files in commonly used software formats, like the one from the commercial package CHEMKIN.

In order to run the simulations, the package REGATH solves the basic conservation equations explained in the chapter 2 through the Newton's Method. Like similar softwares, REGATH reads three main files, containing the chemical mechanism, the thermodynamic parameters and the transport parameters.

The chemical mechanism file enumerates the species involved in the combustion and lists the reactions with their values for A , b and E_a , described in section 2.1, which are used to solve the Arrhenius equation (2.9) for each reaction.

The thermodynamic file contains the 14 polynomial coefficients described in equations 2.34 to 2.36, which determine the values for thermodynamical properties along given $[T_{inf}, T_{med}]$ and $[T_{med}, T_{sup}]$ approximation ranges, for each species involved in the combustion process.

The transport file, as described in Kee *et al.* (2000), lists the species involved in the chemical mechanism and the following parameters:

1. An index indicating whether the molecule has a monatomic, linear or nonlinear geometrical configuration. If the index is 0, the molecule is a single atom. If the index is 1 the molecule is linear, and if it is 2, the molecule is nonlinear.
2. The Lennard-Jones potential well depth ε/k_B in Kelvins.
3. The Lennard-Jones collision diameter σ in Angstroms.
4. The dipole moment β in Debye. Note: a Debye is $10^{-18}cm^3/2erg^{1/2}$.
5. The polarizability α in cubic Angstroms.
6. The rotational relaxation collision number Z_{rot} at 298K.

All those are used to calculate transport properties, as stated in the section 2.3.2.

In the simulations, the package is capable of returning data for the laminar flame speed, flame thickness, maximum temperature and also mass fractions and temperature profiles along the flame.

3.2 Comparison between Kinetic Schemes and Experimental Data

At this stage, schemes from the literature developed for n-butanol and ethanol were compared with data from experiments. A numerical simulation was made, and graphics for laminar flame speed in an one-dimensional premixed flame set were raised.

The selected models for n-butanol were the ones available in the works of Sarathy *et al.* (2009) and Sarathy *et al.* (2012). For ethanol, the schemes of Marinov (1999) and Konnov *et al.* (2011) were the chosen ones, as well as the model of Sarathy *et al.* (2012), which contains the mechanism for ethanol. Data from the experiments described in the works of Sarathy *et al.* (2009), Zhang *et al.* (2013) and Liu *et al.* (2011) was used for n-butanol, and for ethanol, that of the works of Konnov *et al.* (2011) and van Lipzig *et al.* (2011).

The scheme from Sarathy *et al.* (2009) was selected for being quite simple, in the sense that it presents a reduced number of species and reactions, being fast to run in a computer simulation and its code being simple to manipulate. Besides, it was validated experimentally for both premixed flame speed and species concentration profiles, presented in the same article. Data from its experiments was also used for comparison.

The scheme from Sarathy *et al.* (2012) was selected for being more recent than the one from Sarathy *et al.* (2009), and also for presenting the mechanisms for ethanol. It is considered a heavier scheme in terms of computation times, and also harder to manipulate, and was validated for the four butanol isomers.

Along with the experimental data from the work of Sarathy *et al.* (2009), previously cited, data from Liu *et al.* (2011) was also compared, due to the evaluation of flame conditions similar to those presented in both other cited butanol works, but in a different experimental set. The work of Zhang *et al.* (2013) also evaluates the behavior of n-butanol at 353 K and 1 atm, this time, in a combustion bomb.

For ethanol, the scheme of Marinov (1999) was selected for its simplicity, presenting a reduced number of species and reactions, being fast to run in a computer simulation and being its code simple to manipulate. It was also extensively tested, in two experimental sets for flame speed and two others for species concentration profiles.

The work of Konnov *et al.* (2011) was selected for both experimental data and kinetic scheme, for being a more recent ethanol combustion model and for its validation, in a flat-flame laminar burner. Despite being slightly computationally heavier than the model of

Marinov (1999), its simulations did not demand much more time, and its code was also simple to manipulate, at least when compared to that of Sarathy *et al.* (2012).

Finally, the experimental data from the work of van Lipzig *et al.* (2011) was chosen for repeating the experiment of Konnov *et al.* (2011) at the same temperature and pressure, generating very accurate results for laminar flame speed.

3.3 Blends Simulation through Scheme for Butanol Isomers

After having compared schemes, simulations for blends between ethanol and n-butanol were made through the only chosen scheme containing mechanisms for both fuels, the one presented in the work of Sarathy *et al.* (2012).

Blend proportions were set following the volume fractions of butanol in the fuel mixture, from 25 to 25%. Five blends were then evaluated: E100 (0% n-butanol, 100% ethanol), B25 (25% n-butanol, 75% ethanol), B50 (50% n-butanol, 50% ethanol), B75 (75% n-butanol, 25% ethanol) and B100 (100% n-butanol, 0% ethanol).

Graphics for laminar flame speed were then raised, for the ranges of ϕ and conditions described in section 3.1.

3.4 Development and Validation of Combined Scheme for Ethanol + N-Butanol

After analyzing the results of the previous step, it was understood that the scheme of Sarathy *et al.* (2012) was inadequate to the simulation of blends (to be better explained in the next chapter). Then, it was decided that a new scheme for this study should be developed, combining validated schemes for ethanol and n-butanol.

Among the schemes evaluated for both fuels, the one presented in the work of Marinov (1999) for ethanol and the one from Sarathy *et al.* (2009) for n-butanol were chosen for fusion. They are both very fast models, computationally speaking, presenting the lowest number of reactions and species but still keeping a good similarity between the simulated values for laminar flame speed and the experimental data.

As previously cited, kinetic schemes for computer-based simulations normally com-

prise three files: one for the kinetic mechanism, a second for the 14 thermodynamic constants and a third one, presenting values for the calculation of transport properties. In this sense, the fusion of the chosen schemes for ethanol and n-butanol followed the steps:

1. Choice of the skeletal scheme, the one that would keep all of its reactions and species. Computationally speaking, it would be the one whose chemical mechanism's file, thermodynamic file and transport file would base the new scheme. In this case, the first choice was the one from Sarathy *et al.* (2009), for holding the greater number of reactions and species, in the sense that less reactions and species are to be added to the new model and evaluated. It is not the natural choice considering that, hierarchically, the n-butanol schemes were developed based in schemes for simpler alcohols, theoretically producing less deviation; a new scheme using ethanol would be left for a future moment, in case of the first not being validated.
2. Addition of all the reactions from the secondary scheme, in this case, from the one of Marinov (1999). All the reactions from the chemical mechanism's file of Marinov (1999) were added to their equivalents in the work of Sarathy *et al.* (2009).
3. Addition of the new species to the combined model. Those species were the ones present in the mechanism of Marinov (1999) but not present in the one of Sarathy *et al.* (2009). Computationally, the REGATH package returns the information that certain species were not declared in the chemical mechanism's file; they are then manually listed in this file, and data from the thermodynamic file and the transport file from the original model for these certain species are added to the new model.
4. Identification and removal of duplicate reactions. Duplicate reactions are the ones listed twice in the mechanism, identified after the compilation of the combined model; through the chosen method, only the duplicate reactions listed in the skeletal scheme are kept, being the ones from the added scheme removed. These last ones sometimes present different values for the previously described Arrhenius constants. In this case, considering that the reactions from the model of Sarathy *et al.* (2009) were chosen to base the new one, their equivalents from the added scheme must be removed.
5. Numerical analysis and validation of the new model. Through the comparison between the laminar flame speed of the combustion of each fuel in a certain range of fuel-air equivalence ratios and their counterparts from the experiments, the new scheme can be considered fit or unfit for the modeling of the combustion of a certain fuel. In case it is

not considered fit, the process must be repeated, switching the skeletal model.

A graphic representation of what happens in the combination of chemical kinetic schemes is presented in figure 3.1, below.

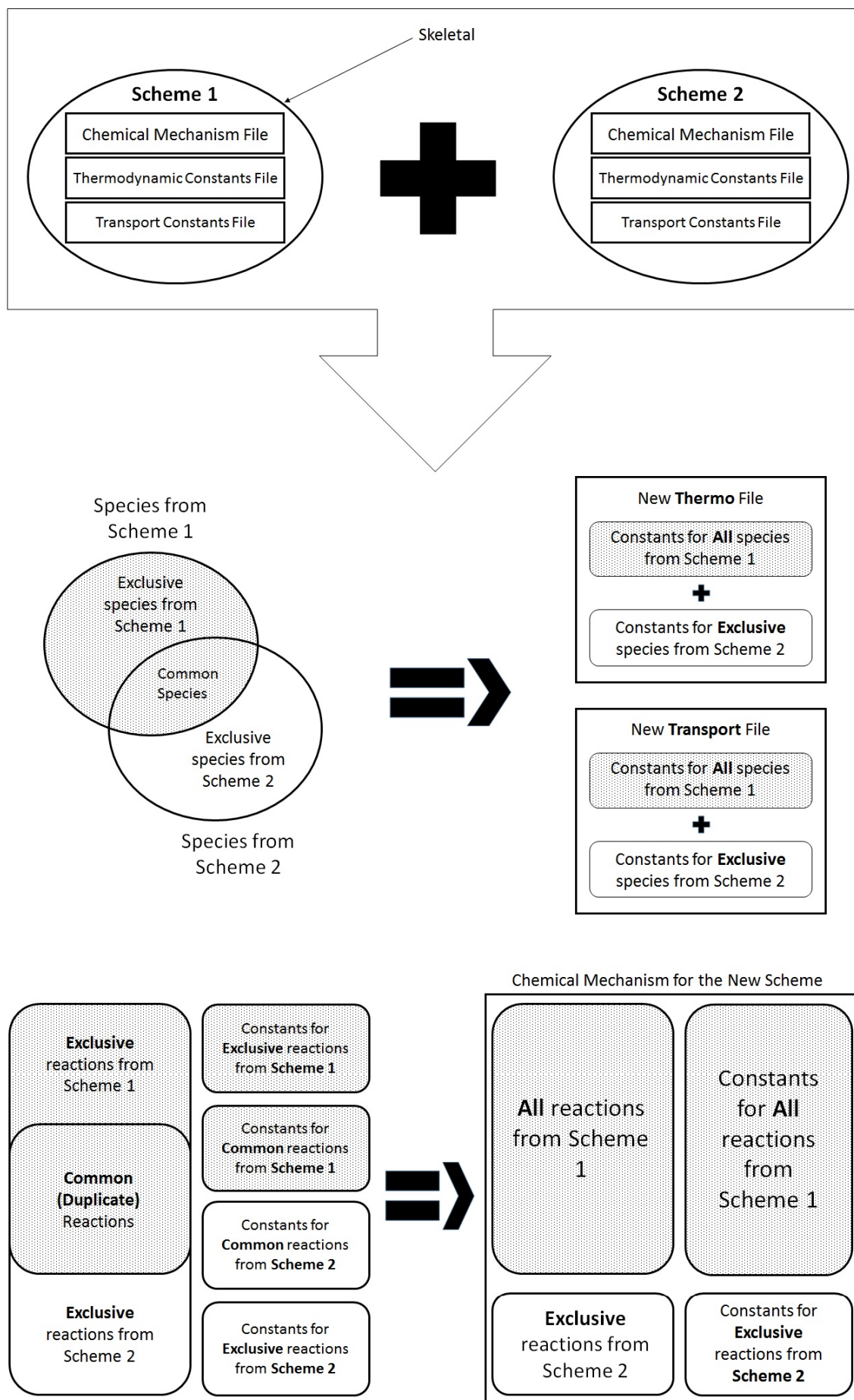


Figure. 3.1: Graphic representation of the fusion of kinetic schemes.

After developing the new chemical scheme, its validation was made. The scheme was tested for laminar flame speed for pure ethanol and pure n-butanol, in a range of fuel-air equivalence ratios of 0.5 to 1.5 for the latter and of 0.5 to 1.4 to the first fuel. As cited, all the simulations were made in a one-dimensional laminar premixed set, at 1 atm, and 353K of temperature for n-butanol and 298K for ethanol. The new model was compared with each of the models used for the fusion, as well as with experimental data from Sarathy *et al.* (2009) and Liu *et al.* (2011) for butanol, as well as that of Konnov *et al.* (2011) and van Lipzig *et al.* (2011) for ethanol.

Due to the good agreement between the new scheme and the experimental data (better explained in the following chapter), no other fusion was made, being the one based on the works of Sarathy *et al.* (2009) (skeletal) and that of Marinov (1999) chosen for the evaluation of the blends.

3.5 Blends Simulation through the New Scheme

After validating the new scheme for each of the pure fuels, theoretical curves for the mixtures between n-butanol and ethanol in a one-dimensional premixed flame set through this scheme were raised.

The theoretical curves for the laminar flame speed for the mixed fuels were raised. The chosen blends were the same from the phase described on section 3.3, E100 (0% n-butanol, 100% ethanol), B25 (25% n-butanol, 75% ethanol), B50 (50% n-butanol, 50% ethanol), B75 (75% n-butanol, 25% ethanol) and B100 (100% n-butanol, 0% ethanol). Flame speed was evaluated for ranges from 0.6 to 1.4. Curves for temperature profiles and species mass concentration for C_2H_5OH (ethanol), C_4H_9OH (n-butanol), O_2 , CO_2 , H_2O and CO were also raised, for the stoichiometric relation, $\phi = 1$. Only the graphics for the pure substances are presented in this step, in order to better show the differences between those fuels.

4 RESULTS AND DISCUSSION

4.1 Comparison between Kinetic Schemes and Experimental Data

Results for the comparison between kinetic schemes and experimental data from the literature, made through the REGATH package, are here presented in graphics, and further, in the appendix A, they are presented in tables.

Information related to the error assessment and experimental and scheme characteristics, as well as input data were previously explained in chapters 2 and 3, respectively. Therefore, they will not be repeated here. It is only important to notice that all values for uncertainties from the experiments were here presented, except for fuel-air equivalence ratios (ϕ), considering their error values are too small to influence final results or even appear in the graphics.

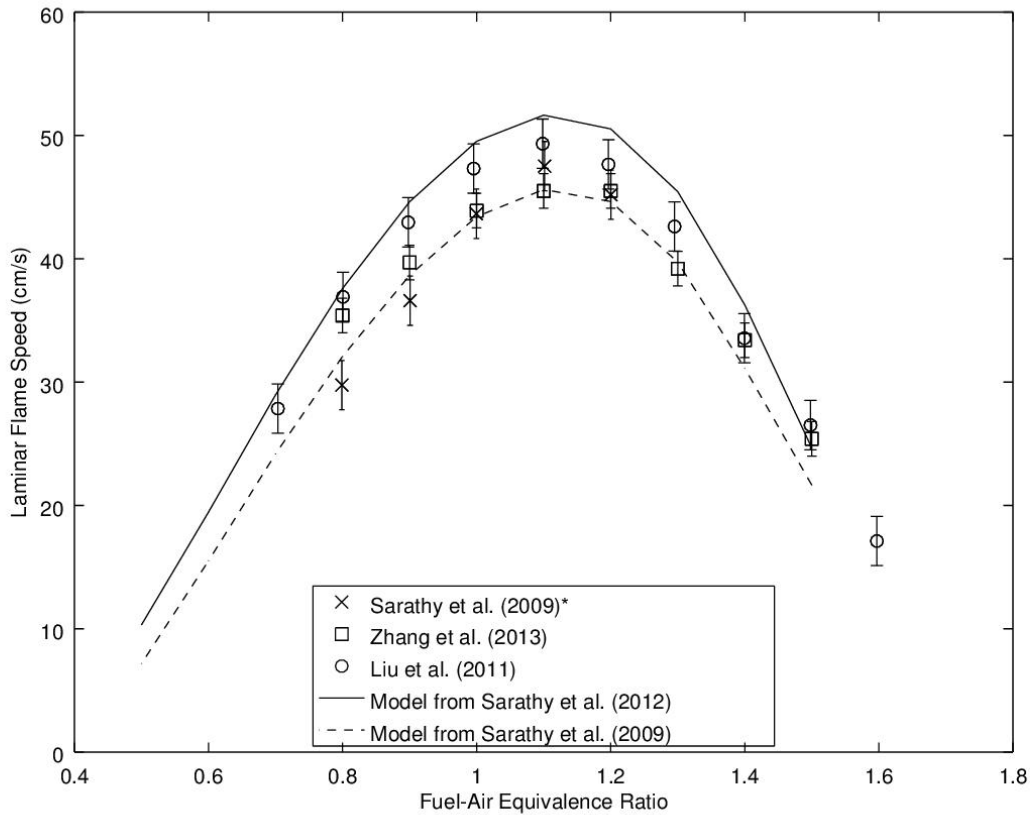


Figure. 4.1: Laminar flame speed of n-butanol/air combustion from various works, $T = 353K$, $p = 1atm$. * Values from Sarathy *et al.* (2009) were evaluated at $T = 350K$ and $p = 0.89atm$.

Figure 4.1 shows the results for n-butanol. By analyzing the graphic, first of all, it

can be seen that the three experiments present quite different results for most equivalence ratios, even for the two ran in the same temperature and pressure conditions, from Liu *et al.* (2011) and Zhang *et al.* (2013). Differences between the experimental methods and types of instruments used, manipulation of the samples, among others may have influenced the final results. Secondly, it can be noticed that both schemes present quite different values when compared with the experiments and between each other. Due to the nature of kinetic schemes, considered a manner to simulate very complex combustion processes, and the differences between the simulated conditions and the real laboratory sets, a certain gap between the values is acceptable.

For n-butanol, both schemes can be considered fit for the representation of its combustion. Standard deviation for the model of Sarathy *et al.* (2009) reached a maximum of 3.8 cm/s, when compared with the experiment of Liu *et al.* (2011), while the model of Sarathy *et al.* (2012) reached a maximum of 6.4 cm/s, when compared with the experiment of Sarathy *et al.* (2009) (being this experiment set in slightly different initial conditions when compared with the others). More data on the errors is presented in section B.2, in appendix A.

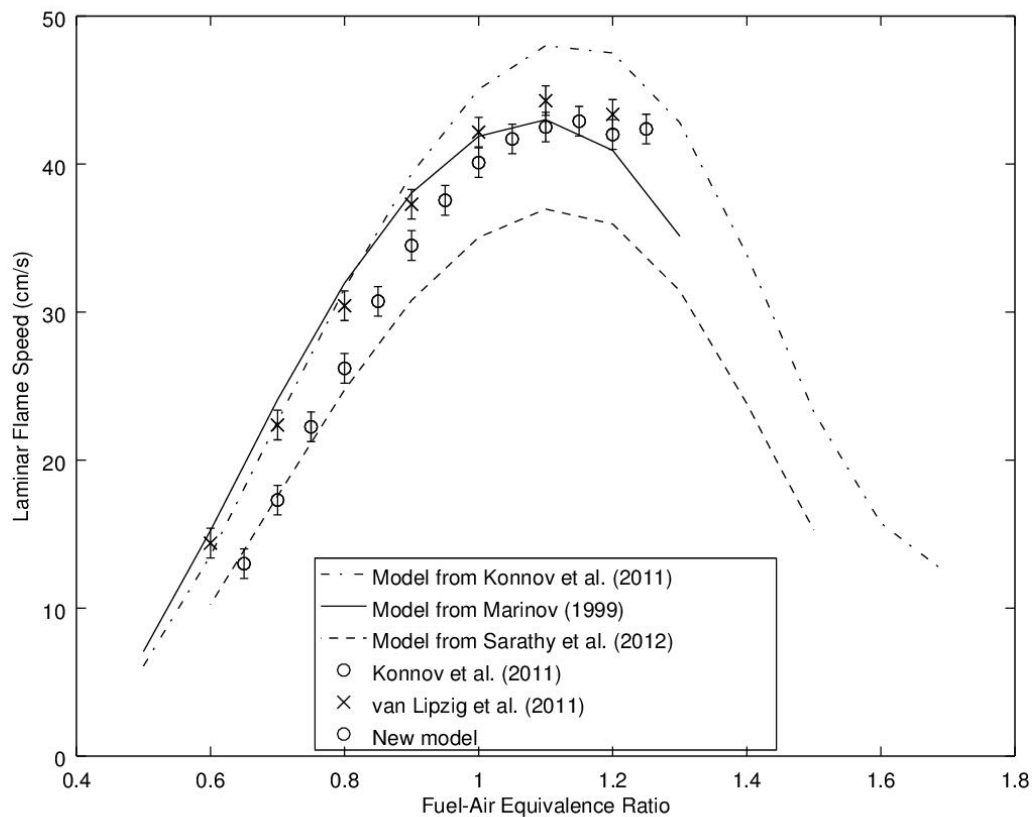


Figure. 4.2: Laminar flame speed of ethanol/air combustion from various works, $T = 298K$, $p = 1atm$.

Figure 4.2 shows the results for ethanol. Experimental values for laminar flame speed, similarly to what happened in the comparison for n-butanol, present differences, even though the experimental conditions are very similar. According to van Lipzig *et al.* (2011), measurements in lower equivalence ratios are affected by flame instabilities in this condition, thus implying that these values may differ. For kinetic schemes, the greatest differences can be seen, specially the one from Sarathy *et al.* (2012), which presents much lower values in comparison with the other schemes and experiments. The schemes from Marinov (1999) and Konnov *et al.* (2011) are very similar for lower equivalence ratios, but differ a lot in higher values; however, the first presents a greater agreement with the experimental data.

For ethanol, the model of Marinov (1999) can be considered very fit for representing the combustion of this fuel, presenting a maximum standard deviation of 4 cm/s, in relation to the experiment from Konnov *et al.* (2011), however, it could not converge for fuel/air equivalence ratios greater than 1.3. The model of Konnov *et al.* (2011) can be considered fairly, but not much adequate to the evaluation, presenting a maximum standard deviation of 5.3 cm/s. On the other hand, the scheme from Sarathy *et al.* (2012) could not be, initially, considered fit for the simulations, because it not only presented a relatively high value for standard deviation in comparison with the experiments (maximum of 6.3 cm/s, in comparison with the one from van Lipzig *et al.* (2011)) but also when compared with the other models, presenting a maximum of 9 cm/s with the one from Konnov *et al.* (2011). Additionally, it can be seen that, while the other two present laminar flame speed values a bit higher than the experimental ones, they are lower for the one from Sarathy *et al.* (2012). It implies that the chosen model, validated for butanol isomers, would not be valid for ethanol.

4.2 Blends Simulation through Scheme for Butanol Isomers

As previously explained, simulations for blends using the scheme from Sarathy *et al.* (2012) were made. The relation between the laminar flame speed of the five blends, namely E100 (0% n-butanol, 100% ethanol), B25 (25% n-butanol, 75% ethanol), B50 (50% n-butanol, 50% ethanol), B75 (75% n-butanol, 25% ethanol) and B100 (100% n-butanol, 0% ethanol), and that of pure ethanol, is presented in figure 4.3.

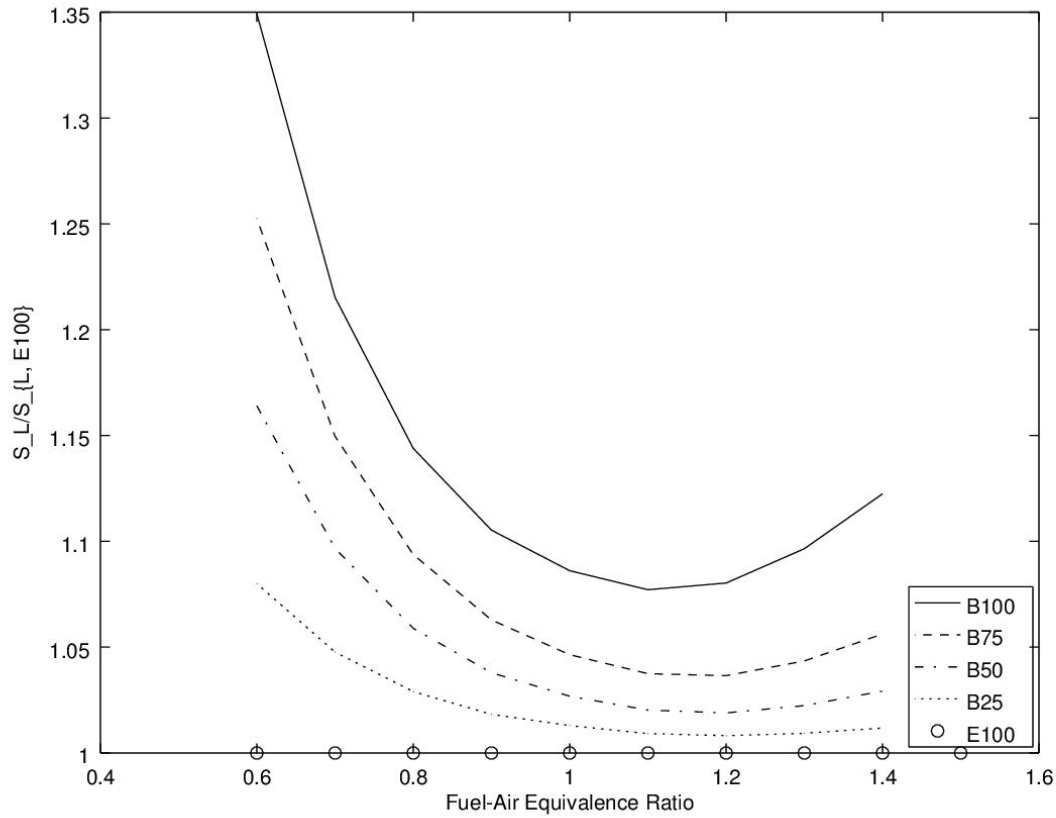


Figure. 4.3: Relation between laminar flame speeds for blends and that of pure ethanol, evaluated through the scheme from Sarathy *et al.* (2012), $T = 298K$, $p = 1atm$.

Due to the lack of experiments for blends between both fuels, simulated results could not be validated. However, by visually analyzing the curves it can be noticed that laminar flame speeds increase by the addition of n-butanol in the mixture, being the curve for n-butanol higher than the one for ethanol. This condition is the opposite of what would be expected for these fuels at atmospheric pressure, as concluded in Broustail *et al.* (2011). In that work both fuels were tested at the same pressure and temperature. It corroborates the conclusion that the scheme from Sarathy *et al.* (2012) is not adequate to the simulation of ethanol and blends between ethanol and n-butanol.

4.3 Development and Validation of Combined Scheme for Ethanol + N-Butanol

For not being considered valid to simulate n-butanol and ethanol at the same time, the scheme from Sarathy *et al.* (2012) was discarded from the present study, and due to the lack

of validated schemes for this condition, a new one was developed for the simulation of ethanol, n-butanol and their blends. As previously explained, this new scheme was created through the fusion of two known kinetic schemes, one for each fuel, namely the one from Marinov (1999) for ethanol and the one from Sarathy *et al.* (2009) for n-butanol. 11 new species and 155 reactions were added. The new scheme presented 129 species and 1033 reactions, being removed duplicates from the mechanism of ethanol. This model was later tested for laminar flame speed for both fuels, then compared with data from experiments from the literature, also with the original schemes and the others previously evaluated.

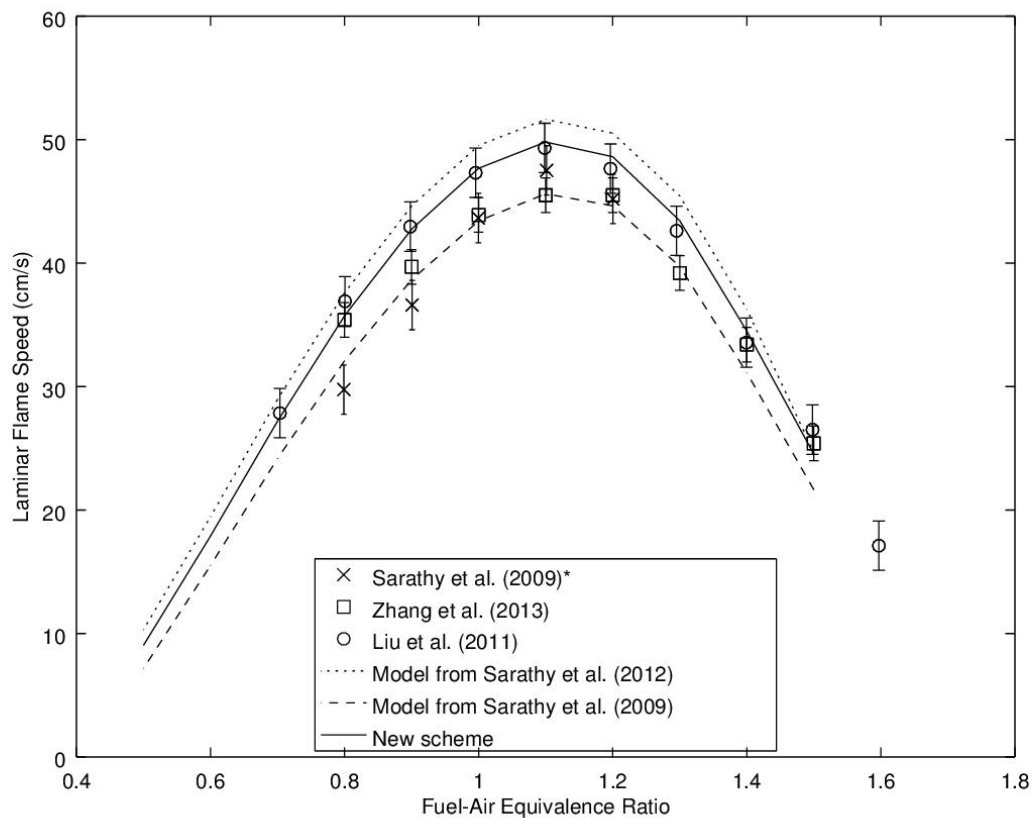


Figure. 4.4: Laminar flame speed of n-butanol/air combustion from previous analysis and the new scheme, $T = 353K$, $p = 1atm$. * Values from Sarathy *et al.* (2009) evaluated at $T = 350K$ and $p = 0.89atm$.

Figure 4.4 shows results for the laminar flame speed of the combustion of n-butanol. The new scheme presents better agreement with experimental results than the previous schemes, specially those of Liu *et al.* (2011), with a standard deviation of 1 cm/s. The greatest difference appears when comparing with speeds measured in the work of Sarathy *et al.* (2009) (standard deviation of 4.6 cm/s), which is not too high. When compared with the other schemes, the

curve for the new one positions itself between the ones from Sarathy *et al.* (2009) and Sarathy *et al.* (2012), presenting a standard deviation of 3.5 and 1.7 cm/s, respectively. Values for laminar flame speed are slightly higher than those from the original scheme, possibly due to reactions present in the scheme for ethanol (Marinov, 1999) that present high heat production rates.

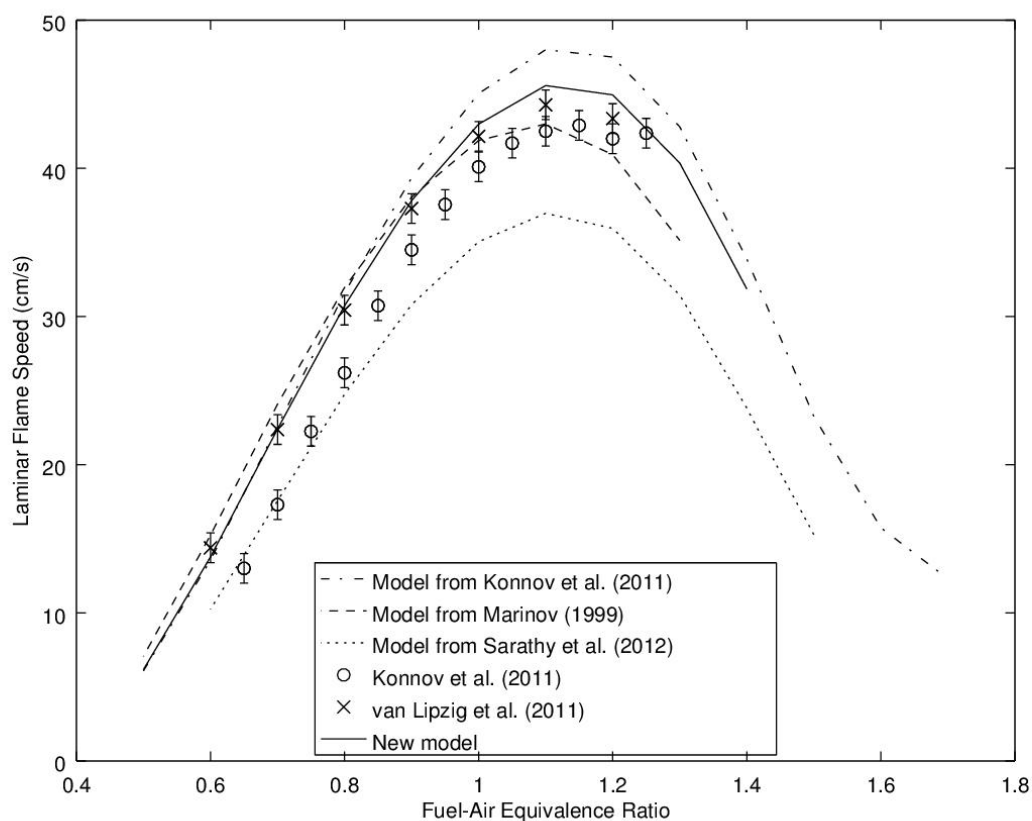


Figure. 4.5: Laminar flame speed of ethanol/air combustion from previous analysis and the new scheme, $T = 298K$, $p = 1atm$.

Figure 4.5 shows results for ethanol. For this fuel, the new scheme presents good agreement with the experimental values, specially with those from the work of van Lipzig *et al.* (2011), presenting a standard deviation of only 0.9 cm/s. The maximum difference is noticed when comparing with data from Konnov *et al.* (2011) (standard deviation of 3.7 cm/s), however, it is the kinetic scheme that presents the closest results when compared with that experiment. When compared with the other models, its curve is positioned between that of (Marinov, 1999) and the one of Konnov *et al.* (2011), being also higher than that from Sarathy *et al.* (2012). New values are also slightly higher than those from the original scheme, possibly due to reactions present in the scheme for n-butanol (Sarathy *et al.*, 2009) that present high

heat production rates, and are activated by the burning of ethanol. Other values for standard deviations are presented in section B.2, in the appendix A.

Considering the results presented here, the new scheme can be considered validated for laminar flame speed for both fuels. This condition theoretically enables the scheme to correctly analyze blends between both fuels.

4.4 Blends Simulation through the New Scheme

After the development and validation of the new scheme for ethanol and n-butanol, the simulations described in section 4.2 were repeated using it. Fuel-air equivalence ratios were set to the range between 0.6 and 1.4 for all blends, and results for laminar flame speed were taken. Additionally, temperature profiles for the stoichiometric proportion (equivalence ratio of 1) were taken, as well as mass fractions of C_2H_5OH (ethanol), C_4H_9OH (n-butanol), O_2 , CO_2 , H_2O and CO , as a function of the temperature. Results are presented in the graphics below.

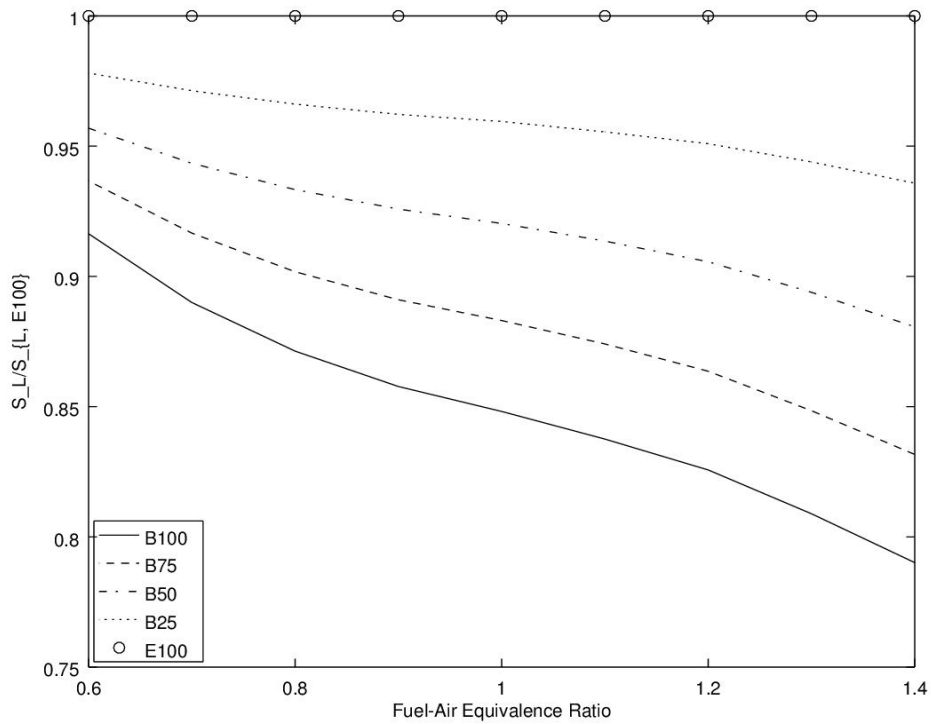


Figure. 4.6: Relation between laminar flame speeds for blends and that of pure ethanol, evaluated through the new scheme, $T = 298K$, $p = 1atm$.

Figure 4.6 relates laminar flame speeds of blends and those of pure ethanol. Values are tabled in section B.1 of the appendix B. By analyzing this graphic it can be seen that ethanol speeds are superior to n-butanol speeds in all equivalence ratios, something also concluded in the work of Broustail *et al.* (2011). Additionally, values for the blends lie proportionally in between the ones for pure fuels, seemingly following the formula:

$$S_L(BX, \phi) = \frac{X}{100} S_L(B100, \phi) + \left(1 - \frac{X}{100}\right) S_L(E100, \phi), \quad (4.1)$$

which is consistent with the results calculated by the REGATH simulations, presenting a standard deviation of 0.2, 0.25 and 0.2 cm/s for B25, B50 and B75, respectively. This relation has yet to be tested, considering that experimental works on mixtures between other kinds of fuels present non linear relations (Broustail *et al.*, 2011).

The influence of the molecular formula in the laminar flame speed of pure fuels is a much studied subject. Reynolds and Gerstein (1948), as cited in Coelho and Costa (2012), investigated this relation for alkanes ($C_n H_{2n+2}$), alkenes ($C_n H_{2n}$) and alkynes ($C_n H_{2n-2}$), stating that for the latter two groups, the lower the number of carbon atoms, the higher the flame speed, while for the first, they could not notice any significant variation. Perhaps for alcohols with such a difference in the number of carbon atoms (4 for n-butanol and 2 to ethanol) this characteristic plays an important role, explaining the behavior identified in this and other (Broustail *et al.*, 2011) studies. However, as affirmed in the work of Coelho and Costa (2012), thermal diffusivity and flame temperature have a much greater influence in this characteristic, therefore, this study cannot jump to final conclusions on this issue.

Figures 4.7 to 4.12 present values for temperature profiles as a function of the distance from the center of the flame (x [mm]) and mass fractions for the selected species for the combustion of pure n-butanol and ethanol. The fuel/air equivalence ratio is one (stoichiometric combustion) for all graphics.

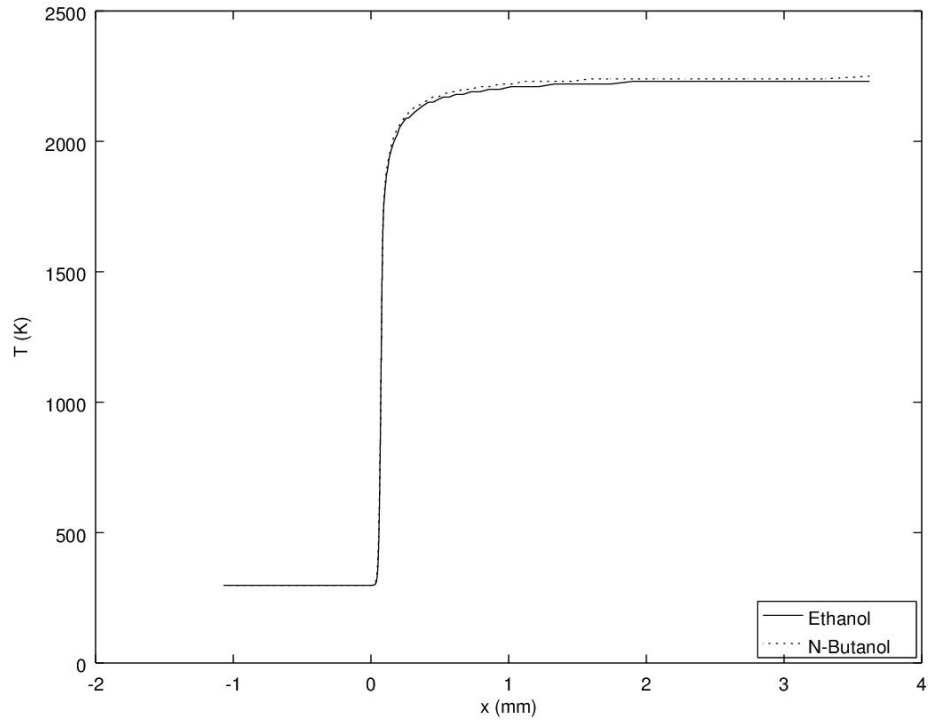


Figure. 4.7: Temperature profile for B100 and E100, $T_0 = 298K$, $p = 1atm$.

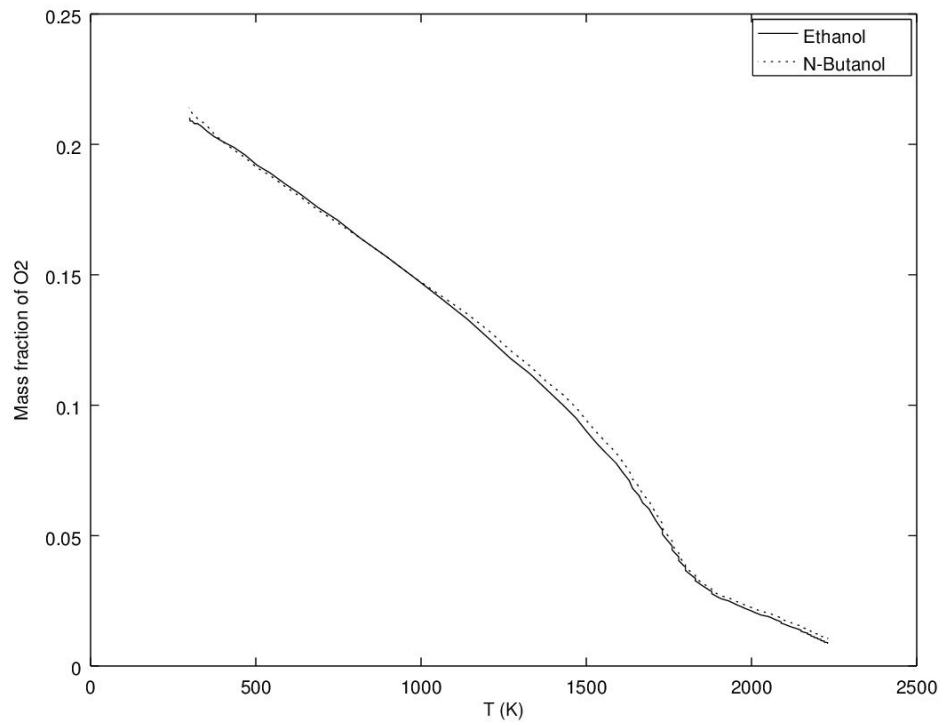


Figure. 4.8: Mass fraction of O_2 , $T_0 = 298K$, $p = 1atm$.

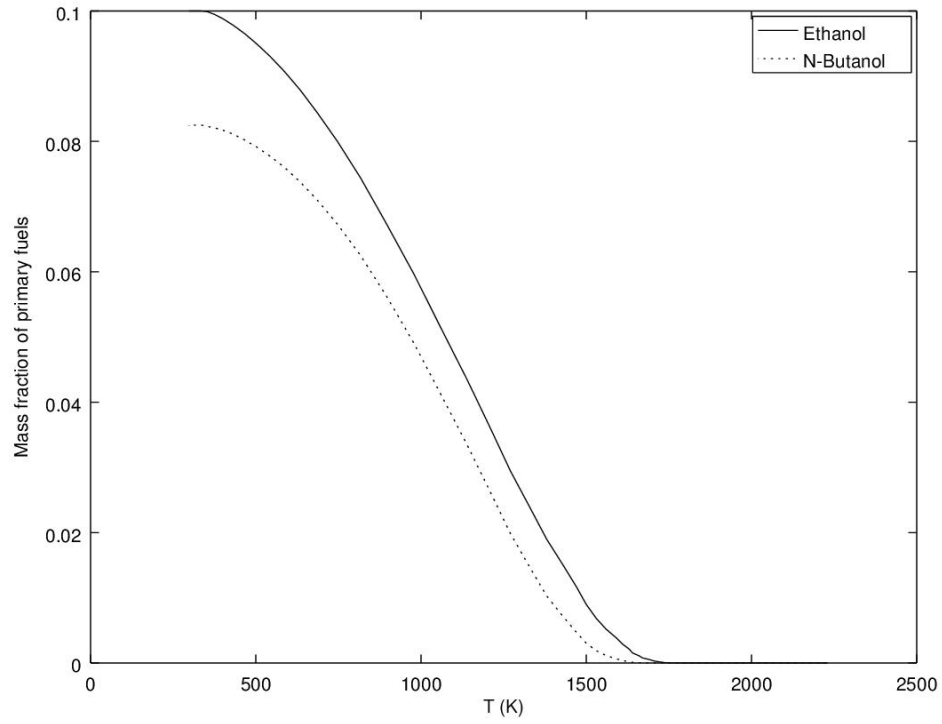


Figure. 4.9: Mass fractions of pure fuels (ethanol and n-butanol), $T_0 = 298K$, $p = 1atm$.

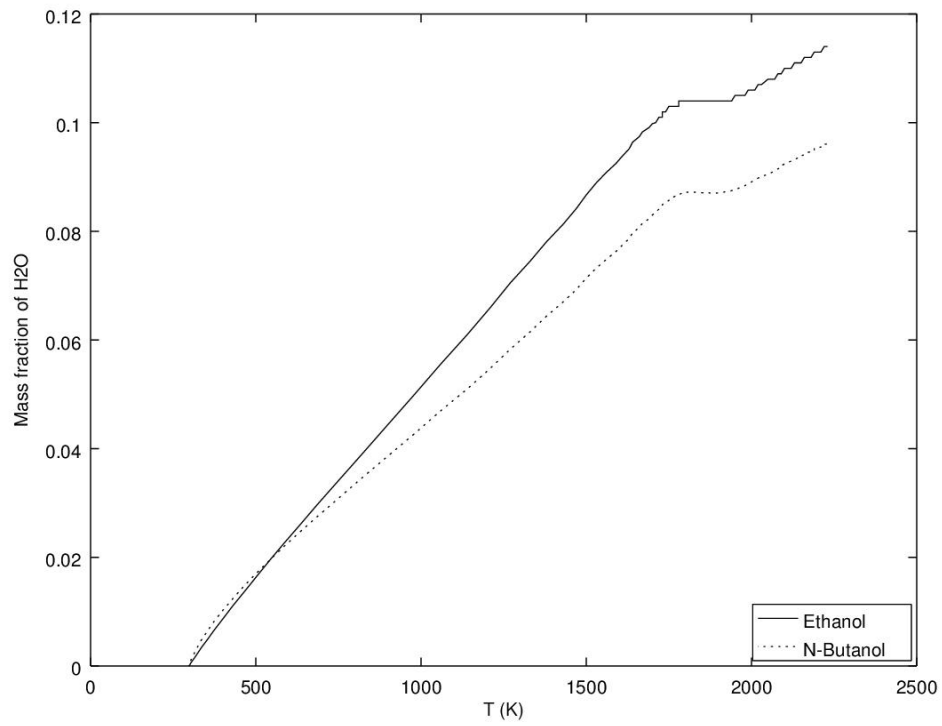


Figure. 4.10: Mass fraction of H_2O , $T_0 = 298K$, $p = 1atm$.

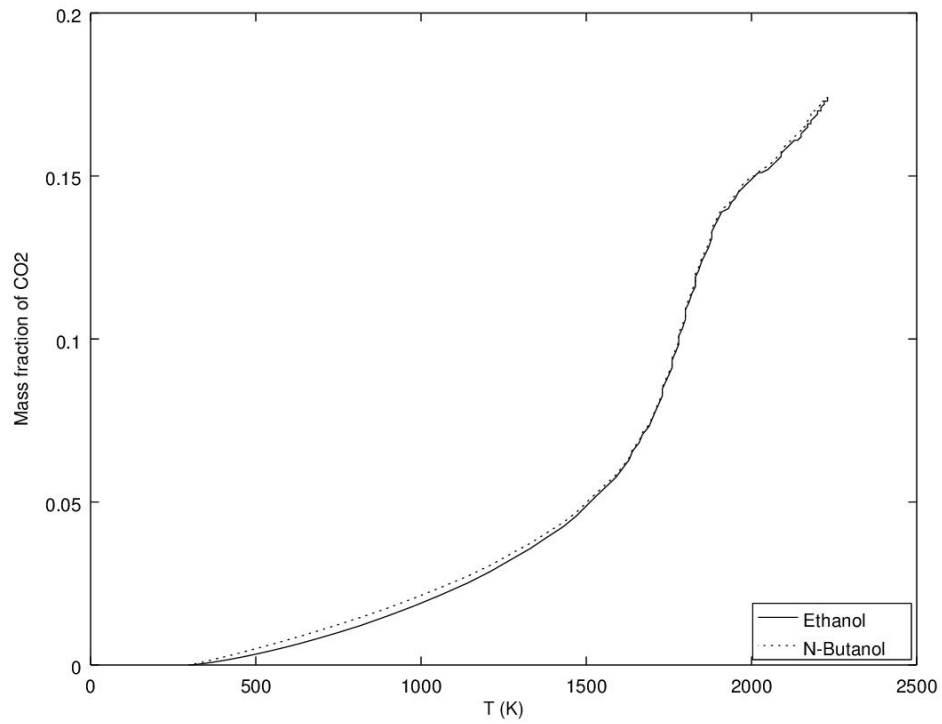


Figure. 4.11: Mass fraction of CO_2 , $T_0 = 298\text{K}$, $p = 1\text{atm}$.

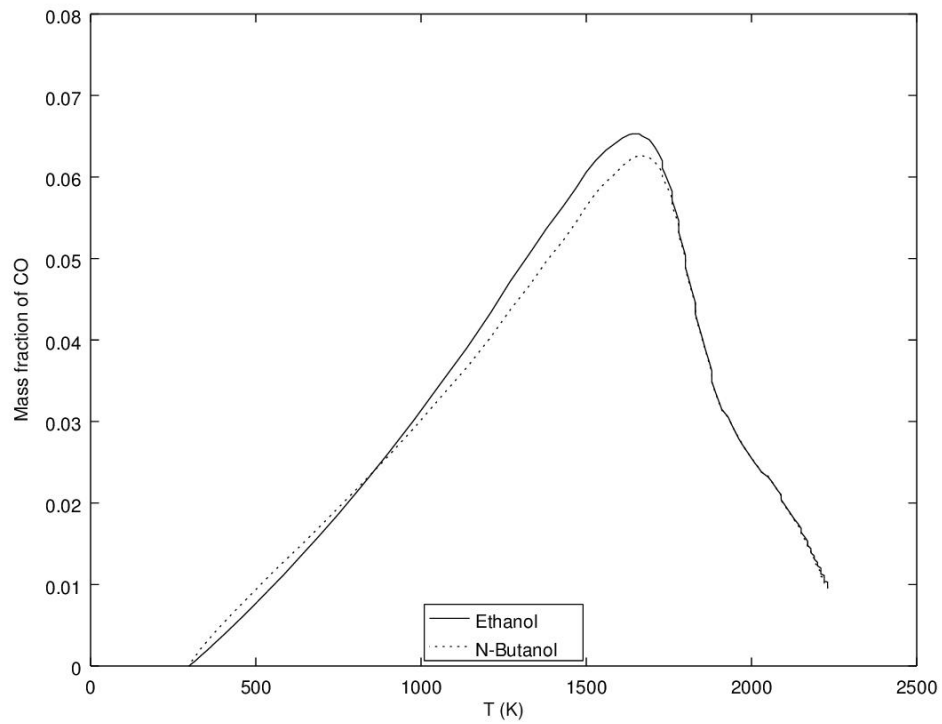


Figure. 4.12: Mass fraction of CO , $T_0 = 298\text{K}$, $p = 1\text{atm}$.

The figures 4.7 to 4.12 show some characteristics of the burning of ethanol and n-butanol. First of all, n-butanol presents a slightly higher maximum temperature (2245 K), being considered a hotter flame when compared to the one of ethanol (2234 K). This characteristic might provoke slightly higher NO_X emissions, at least the thermal produced (Turns, 2012), but this condition cannot be verified due to the absence of those species in the new kinetic scheme. It can also be seen that the flame of pure n-butanol reaches its maximum temperature value at a longer distance from the center of the simulated geometry than that of pure ethanol, perhaps indicating that the previous is a slower flame (corroborating the conclusions from the graphics for laminar flame speed). The graphics for mass fractions, on the other hand, show clearly the differences in the production of water between the combustion of n-butanol and ethanol, being higher for the latter. Additionally, they show that n-butanol presents a delayed and lower production of CO, also showing its peak at a higher temperature than that of ethanol, which may affect emissions of this gas. Finally, it can be seen that the consumption behaviors of the fraction of pure fuels differ, considering that the ethanol fraction is only fully consumed at a higher temperature than that of n-butanol. These graphics were plotted as a function of the temperature T , due to the temperature-dependency in the formation of species; besides, due to the scale of the temperature and species formation profiles, restricted to a very small interval in the x axis, this kind of graphic was considered more illustrative of the parameters of interest.

Data evaluated for the mixtures in these conditions, as stated before, could not be verified with experiments, due to the lack of studies for blends between the two fuels. Additionally, experiments for the pure fuels were done in configurations not reproduced in the present study, both in terms of flame set, fuel-air equivalence ratios, pressure and initial temperature.

5 CONCLUSIONS AND FUTURE WORK PERSPECTIVES

5.1 Conclusions

Kinetic schemes available in the literature for ethanol and n-butanol were compared to experimental data for laminar flame speed in a one-dimensional premixed flame configuration, being validated or not. For n-butanol, both schemes, the one presented in the work of Sarathy *et al.* (2012) and that of Sarathy *et al.* (2009), presented good agreement with experiments described in the literature, presenting maximum standard deviations of 6.42 cm/s (compared to different pressures and temperature) and 3.82 cm/s, respectively, when compared to the experiments of Sarathy *et al.* (2009) and Liu *et al.* (2011). For ethanol, the models from the works of Marinov (1999) presented good agreement with experiments, showing maximum standard deviations of 4.01 cm/s, while the one from Konnov *et al.* (2011) showed a fair agreement, with a maximum standard deviations of 5.26 cm/s, both when compared to data from the work of Konnov *et al.* (2011). The model of Sarathy *et al.* (2012) could not present a good agreement for ethanol, not only because of its uncertainty values (maximum standard deviation of 6.25 cm/s when compared to the speeds from van Lipzig *et al.* (2011)) but also for presenting speeds much lower than those of the other schemes. This conclusion was corroborated by the fact that the simulated curve for pure ethanol was positioned lower than that of pure n-butanol at the same pressures and initial temperatures, which is the opposite of what is found in reported experiments in the literature (Broustail *et al.*, 2011). Therefore, it can be concluded that the scheme of Sarathy *et al.* (2012) is not fit for the evaluation of blends, being discarded from further evaluations.

Due to the lack of simple combined schemes for both ethanol and n-butanol, a new one was developed, combining the reactions and properties from the validated models of Marinov (1999) for the first fuel and of Sarathy *et al.* (2009) for the latter. Curves for laminar flame speed presented good agreement with the values from experiments reported in the literature, presenting a maximum standard deviation of 3.75 cm/s for ethanol and 3.00 cm/s for n-butanol. The new scheme was then used for the simulation of blends between both fuels, presenting curves in positions that agree with experiments. Additionally, theoretical curves for temperature profiles and species mass fractions were raised, presenting variations in the behavior of the

mixture depending on the fraction of each pure fuel.

The work presented here fulfilled its initial objectives, being able to raise data for the behavior of mixtures between ethanol and n-butanol through a validated model. The manipulation of kinetic schemes was able to produce a new model that could precisely define laminar flame speeds for both pure fuels. It is important to notice that, in this case, the fusion of schemes showed flame speeds that were higher than those of the original models, possibly due to the high number of common reactions (228, or 60% of the scheme of Marinov (1999)) and species (46, or 81% of those of Marinov (1999)). Perhaps the number of new reactions for the original species also influenced the behavior of n-butanol, changing the rates of production of these species and, thus, changing the flame speed. Further works should explore the chemical behavior of the fusion of kinetic schemes in a deeper approach.

5.2 Future work perspectives

The present work intended to begin studies on the combustion of mixtures between two biofuels, ethanol and n-butanol. Results obtained here perhaps raise more questions than answers. The combustion behavior of each of the fuels, in their pure form, is not yet well understood, therefore, there is a long way to go until a good comprehension of the burning behavior of their mixtures. Additionally, the manipulation of kinetic schemes is not an exact science, and different methods of combining models may present very different results. Some suggested themes for future studies are:

- To run experiments on the combustion of both pure fuels and their mixtures, in the same configurations, in order to raise data for laminar flame speed, species mass fractions (in JSR, for example), ignition characteristics, quenching, among others, enabling a more complete validation of the scheme developed in the present work and others to be developed further;
- To add and evaluate mechanisms for other substances to the kinetic scheme, such as NO and NO_X (pollutant emissions) and/or CH^* and OH^* (involved in light emissions);
- To validate the chemical scheme previously developed in other flame configurations, such as laminar counterflow diffusion flames or even turbulent flames;

- To add other fuels to the kinetic scheme, such as gasoline, diesel and biodiesel surrogates, developing a broader scheme, to be validated.
- To broaden the research on kinetic schemes, developing and validating new schemes for both fuels, based on other models available in the literature, or to run detailed studies on the behavior of the reactions involved in the burning of each pure fuel, finding new ones and improving the known reactions;
- To better study the chemical interaction between ethanol and n-butanol, not only in terms of solubility but also changes in the physicochemical behavior of the mixture;
- To develop methods for the combination of kinetic schemes, preserving original characteristics or calibrating it in order to correctly simulate the actual behavior of the combustion of more than one fuel.

Bibliography

Key World Energy Statistics 2015. International Energy Agency; OECD, 2015.

AFDC. Global ethanol production. 2016.

AGARWAL, A.K. Biofuels (alcohols and biodiesel) applications as fuels for internal combustion engines. **Progress in Energy and Combustion Science**, v. 33, n. 3, 233 – 271, 2007.

ALVISO, D.; ROLON, J.; SCOUFLAIRE, P. and DARABIHA, N. Experimental and numerical studies of biodiesel combustion mechanisms using a laminar counterflow spray premixed flame. **Fuel**, v. 153, n. 0, 154 – 165, 2015.

BERGTHORSON, J.M. and THOMSON, M.J. A review of the combustion and emissions properties of advanced transportation biofuels and their impact on existing and future engines. **Renewable and Sustainable Energy Reviews**, v. 42, n. 0, 1393 – 1417, 2015.

BROUSTAIL, G.; SEERS, P.; HALTER, F.; MORÉAC, G. and MOUNAIM-ROUSSELLE, C. Experimental determination of laminar burning velocity for butanol and ethanol iso-octane blends. **Fuel**, v. 90, n. 1, 1 – 6, 2011.

URL: <http://www.sciencedirect.com/science/article/pii/S0016236110004928>

COELHO, P. and COSTA, M. **Combustão**. Orion, Lisbon, Portugal, 2nd ed., 2012.

DAGAUT, P.; SARATHY, S. and THOMSON, M. A chemical kinetic study of n-butanol oxidation at elevated pressure in a jet stirred reactor. **Proceedings of the Combustion Institute**, v. 32, n. 1, 229 – 237, 2009.

URL: <http://www.sciencedirect.com/science/article/pii/S1540748908000151>

DARABIHA, N.; ESPOSITO, E.; LACAS, F. and VEYNANTE, D. **Combustion**. Ecole Centrale Paris, Paris, France, 2006.

DEMIRBAS, A. Progress and recent trends in biofuels. **Progress in Energy and Combustion Science**, v. 33, n. 1, 1 – 18, 2007.

URL: <http://www.sciencedirect.com/science/article/pii/S0360128506000256>

DIAS, M.O.; JUNQUEIRA, T.L.; JESUS, C.D.; ROSSELL, C.E.; FILHO, R.M. and BONOMI, A. Improving second generation ethanol production through optimization of first generation production process from sugarcane. **Energy**, v. 43, n. 1, 246 – 252, 2012. 2nd International Meeting on Cleaner Combustion (CM0901-Detailed Chemical Models for Cleaner Combustion).

URL: <http://www.sciencedirect.com/science/article/pii/S0360544212003325>

DIAS, M.O.; PEREIRA, L.G.; JUNQUEIRA, T.L.; PAVANELLO, L.G.; CHAGAS, M.F.; CAVALETT, O.; FILHO, R.M. and BONOMI, A. Butanol production in a sugarcane biorefinery using ethanol as feedstock. part i: Integration to a first generation sugarcane distillery. **Chemical Engineering Research and Design**, v. 92, n. 8, 1441 – 1451, 2014. Green Processes and Eco-technologies - Focus on Biofuels.

ELLABBAN, O.; ABU-RUB, H. and BLAABJERG, F. Renewable energy resources: Current status, future prospects and their enabling technology. **Renewable and Sustainable Energy Reviews**, v. 39, 748 – 764, 2014.

URL: <http://www.sciencedirect.com/science/article/pii/S1364032114005656>

FOX, R.; MCDONALD, A. and PRITCHARD, P. **Introdução à mecânica dos fluidos**. LTC, 6th ed., 2006.

HEYWOOD, J. **Internal Combustion Engine Fundamentals**. McGraw-Hill Education, 1988.

JIN, C.; YAO, M.; LIU, H.; FON F. LEE, C. and JI, J. Progress in the production and application of n-butanol as a biofuel. **Renewable and Sustainable Energy Reviews**, v. 15, n. 8, 4080 –

4106, 2011.

JIN, H.; CUOCI, A.; FRASSOLDATI, A.; FARAVELLI, T.; WANG, Y.; LI, Y. and QI, F. Experimental and kinetic modeling study of {PAH} formation in methane coflow diffusion flames doped with n-butanol. **Combustion and Flame**, v. 161, n. 3, 657 – 670, 2014. Special Issue on Alternative Fuels.

URL: <http://www.sciencedirect.com/science/article/pii/S0010218013003945>

KEE, R.J.; RUPLEY, F.M.; MILLER, J.A.; COLTRIN, M.E.; GRACAR, J.F.; MEEKS, E.; MOFFAT, H.K.; LUTZ, A.E.; DIXONLEWIS, G.; SMOOKE, M.D.; WARNATZ, J.; G. H. EVANS, R.S.L.; MITCHELL, R.E.; PETZOLD, L.R.; REYNOLDS, W.C.; CARACOTSIOS, M.; STEWART, W.E.; GLARBORG, P.; WANG, C. and ADIGUN, O. **Chemkin Collection**. 2000. Release 3.6.

KONNOV, A.; MEUWISSEN, R. and DE GOEY, L. The temperature dependence of the laminar burning velocity of ethanol flames. **Proceedings of the Combustion Institute**, v. 33, n. 1, 1011 – 1019, 2011.

LEPLAT, N.; DAGAUT, P.; TOGBÉ, C. and VANDOOREN, J. Numerical and experimental study of ethanol combustion and oxidation in laminar premixed flames and in jet-stirred reactor. **Combustion and Flame**, v. 158, n. 4, 705 – 725, 2011. Special Issue on Kinetics.

URL: <http://www.sciencedirect.com/science/article/pii/S0010218010003627>

LIU, W.; KELLEY, A.P. and LAW, C.K. Non-premixed ignition, laminar flame propagation, and mechanism reduction of n-butanol, iso-butanol, and methyl butanoate. **Proceedings of the Combustion Institute**, v. 33, n. 1, 995 – 1002, 2011.

MAN, X.; TANG, C.; ZHANG, J.; ZHANG, Y.; PAN, L.; HUANG, Z. and LAW, C.K. An experimental and kinetic modeling study of n-propanol and i-propanol ignition at high temperatures. **Combustion and Flame**, v. 161, n. 3, 644 – 656, 2014. Special Issue on Alternative Fuels.

URL: <http://www.sciencedirect.com/science/article/pii/S0010218013002976>

MARINOV, N. A detailed chemical kinetic model for high temperature ethanol oxidation. **International Journal of Chemical Kinetics**, v. 31, n. 2-3, 183–220, 1999.

MONCHICK, L. and MASON, E. Transport properties of polar gases. **Vacuum**, v. 12, n. 1, 53–, 1962.

URL: <http://www.sciencedirect.com/science/article/pii/0042207X62909582>

RAU, F.; HARTL, S.; VOSS, S.; STILL, M.; HASSE, C. and TRIMIS, D. Laminar burning velocity measurements using the heat flux method and numerical predictions of iso-octane/ethanol blends for different preheat temperatures. **Fuel**, v. 140, 10 – 16, 2015.

URL: <http://www.sciencedirect.com/science/article/pii/S0016236114009284>

REYNOLDS, T.W. and GERSTEIN, M. Influence of molecular structure of hydrocarbons on rate of flame propagation. **Symposium on Combustion and Flame, and Explosion Phenomena**, v. 3, n. 1, 190 – 194, 1948.

URL: <http://www.sciencedirect.com/science/article/pii/S1062289649800250>

ROSILLO-CALLE, F. and CORTEZ, L.A. Towards proalcohol ii—a review of the brazilian bioethanol programme. **Biomass and Bioenergy**, v. 14, n. 2, 115 – 124, 1998.

URL: <http://www.sciencedirect.com/science/article/pii/S0961953497100204>

SARATHY, S.; THOMSON, M.; TOGBÉ, C.; DAGAUT, P.; HALTER, F. and MOUNAIM-ROUSSELLE, C. An experimental and kinetic modeling study of n-butanol combustion. **Combustion and Flame**, v. 156, n. 4, 852 – 864, 2009.

SARATHY, S.M.; VRANCKX, S.; YASUNAGA, K.; MEHL, M.; OßWALD, P.; METCALFE, W.K.; WESTBROOK, C.K.; PITZ, W.J.; KOHSE-HÖINGHAUS, K.; FERNANDES, R.X. and CURRAN, H.J. A comprehensive chemical kinetic combustion model for the four butanol isomers. **Combustion and Flame**, v. 159, n. 6, 2028 – 2055, 2012.

SU, Y.; ZHANG, P. and SU, Y. An overview of biofuels policies and industrialization in the major biofuel producing countries. **Renewable and Sustainable Energy Reviews**, v. 50, 991

– 1003, 2015.

URL: <http://www.sciencedirect.com/science/article/pii/S1364032115003020>

TURNER, S. **An introduction to combustion : concepts and applications**. McGraw-Hill, New York, third ed., 2012.

VAN LIPZIG, J.; NILSSON, E.; DE GOEY, L. and KONNOV, A. Laminar burning velocities of n-heptane, iso-octane, ethanol and their binary and tertiary mixtures. **Fuel**, v. 90, n. 8, 2773 – 2781, 2011.

URL: <http://www.sciencedirect.com/science/article/pii/S0016236111002365>

ZHANG, X.; TANG, C.; YU, H.; LI, Q.; GONG, J. and HUANG, Z. Laminar flame characteristics of iso-octane/n-butanol blend–air mixtures at elevated temperatures. **Energy & Fuels**, v. 27, n. 4, 2327–2335, 2013.

URL: <http://dx.doi.org/10.1021/ef4001743>

ZHOU, H.; SU, Y. and WAN, Y. Phase separation of an acetone–butanol–ethanol (abe)–water mixture in the permeate during pervaporation of a dilute {ABE} solution. **Separation and Purification Technology**, v. 132, 354 – 361, 2014.

URL: <http://www.sciencedirect.com/science/article/pii/S1383586614003463>

APENDIX A – Conservation Equations for Laminar Reacting Flows

Along with the chemical kinetics of combustion processes, to take into account the particularities of the flow, in terms of thermodynamics and fluid mechanics, is also important to understand it. Combustion is a very complex phenomenon, therefore, in order to be able to describe it mathematically it is necessary to simplify its formulation to an easier form.

The conservation equations are the ones able to describe complex flow phenomena in the fields of thermodynamics and fluid mechanics. For the purposes of the present work, considering the flame set and the computational tools used in the project, it is interesting to treat the combustion in one particular situation: a steady flow for a one-dimensional planar geometry, as seen in the figure A.1.

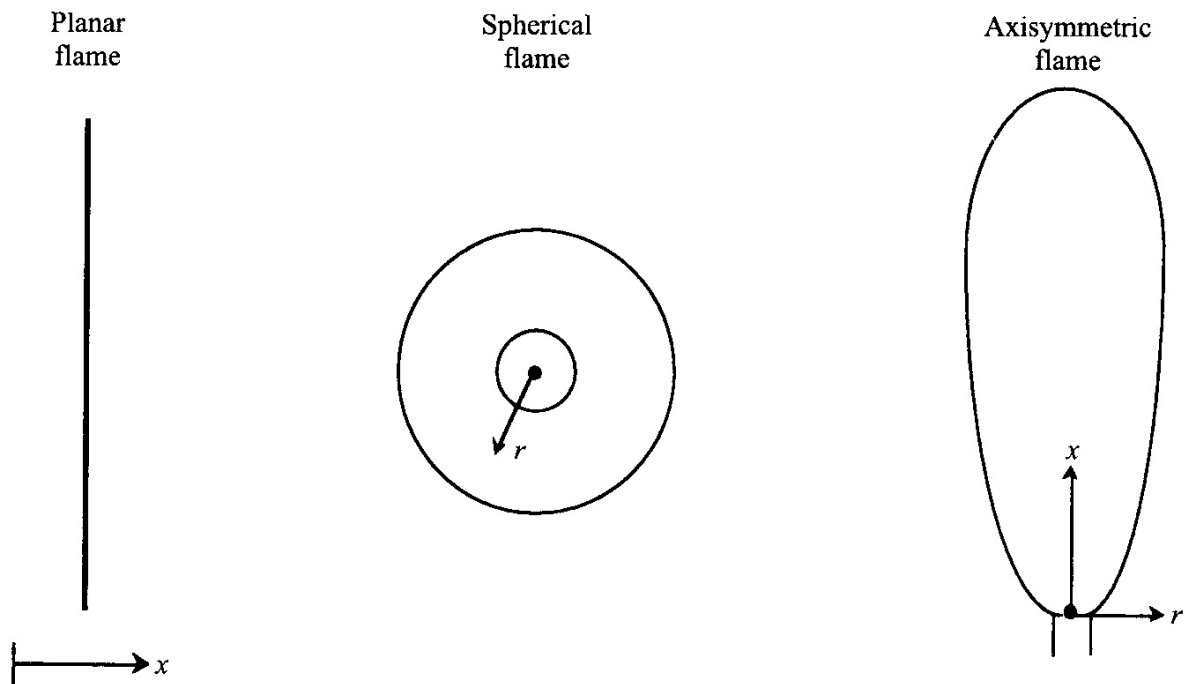


Figure. A.1: Coordinate systems for planar flames, spherically symmetric flames (droplet burning) and axisymmetric flames (jet flames). Source: Turns (2012).

It is important to notice that this formulation is not valid for turbulent flows, due to complex, multicomponent diffusion that affects the flame propagation (Turns, 2012). For the present work, however, the physics of the studied phenomenon, the laminar flame, can be easily captured by the following equations. The theory here described is the one available in the

Chapter 7 of Turns (2012).

A.1 Mass Conservation

In a general form, considering the flow in a determinate control volume, mass variations can be understood as density variations as function of time and space, as stated in equation A.1:

$$\frac{d\rho}{dt} + \nabla \cdot (\rho V) = 0, \quad (\text{A.1})$$

for t the time, ρ the local density and V the velocity vector.

In a unidimensional, axial form, the equation A.1 can be considered:

$$\frac{d\rho}{dt} = -\frac{\partial(\rho v_x)}{\partial x}, \quad (\text{A.2})$$

for ρ the local density, v_x the axial velocity and x the axial distance. In the case of steady flow, $d\rho/dt = 0$,

$$\frac{\partial(\rho v_x)}{\partial x} = 0, \quad (\text{A.3})$$

or

$$\rho v_x = \text{constant}. \quad (\text{A.4})$$

For the case of a spheric flame, for example, a formulation for a spherical coordinate system is given by:

$$\frac{1}{r^2} \frac{\partial}{\partial r}(r^2 \rho v_r) + \frac{1}{r \sin \theta} \frac{\partial}{\partial \theta}(\rho v_\theta \sin \theta) + \frac{1}{r \sin \theta} \frac{\partial(\rho v_\phi)}{\partial \phi} = 0, \quad (\text{A.5})$$

which, simplifying for a 1-D spherically symmetric system, in which $v_\theta = v_\phi = 0$, and the operators $\partial/\partial\theta = \partial/\partial\phi = 0$, the equation A.5 becomes:

$$\frac{1}{r^2} \frac{d}{dr}(r^2 \rho v_r) = 0, \quad (\text{A.6})$$

or

$$r^2 \rho v_r = \text{constant}. \quad (\text{A.7})$$

A.2 Species Conservation

The theory behind the species conservation is quite complex, and can be better understood in the chapters 3 and 7 of the work of Turns (2012). In a general form, the vector form for mass conservation of the i th species can be expressed by:

$$\underbrace{\frac{\partial(\rho Y_i)}{\partial t}}_{\text{Rate of gain of mass of species } i \text{ per unit volume}} + \underbrace{\nabla \cdot \dot{m}_i''}_{\text{Net rate of mass flow of species } i \text{ out by diffusion and bulk flow per unit volume}} = \underbrace{\dot{m}_i'''}_{\text{Net rate of mass production of species } i \text{ per unit volume}} \quad \text{for } i = 1, 2, \dots, N, \quad (\text{A.8})$$

for Y_i the mass concentration of the species and m_i its mass. Bulk flow is the flux of the biggest part of the mixture. The mass flux of i , \dot{m}_i'' , can be defined as:

$$\dot{m}_i'' \equiv \rho Y_i v_i, \quad (\text{A.9})$$

in which ρ is the density and v_i is the species velocity. This value is composed by the bulk velocity, V , and its diffusion velocity, $v_{i,diff}$, in the form:

$$v_i = V + v_{i,diff}. \quad (\text{A.10})$$

$v_{i,diff}$ depends on the diffusion mode that happens in the flow, being a function of diffusivity. Finally, the equation A.8 can be rewritten as:

$$\frac{\partial(\rho Y_i)}{\partial t} + \nabla \cdot [\rho Y_i (V + v_{i,diff})] = \dot{m}_i''', \quad \text{for } i = 1, 2, \dots, N. \quad (\text{A.11})$$

A.3 Momentum Conservation

Turns (2012) presents a complete and very intricate explanation for the momentum conservation in the chapter 7 of its work, however, it does not present a general form. On the other hand, the work of Coelho and Costa (2012) presents this form in a different notation. Summarizing, it defines the momentum conservation equation as:

$$\rho \frac{\partial \vec{v}}{\partial t} + \rho \vec{v} \cdot \nabla \vec{v} = -\nabla p + \nabla \cdot [\mu [\nabla \vec{v} + (\nabla \vec{v})^T]] - \frac{2}{3} \mu (\nabla \cdot \vec{v}) \vec{I} + \rho \vec{g}, \quad (\text{A.12})$$

for \vec{v} the velocity vector, ρ the density, ∇ the vector differential operator, μ the viscosity, \vec{I} the identity tensor and \vec{g} the gravity vector. The vectors are given by:

$$\vec{v} = v_x \hat{i} + v_y \hat{j} + v_z \hat{k} = v_r \hat{e}_r + v_\theta \hat{e}_\theta + v_z \hat{k} = v_r \hat{e}_r + v_\theta \hat{e}_\theta + v_\phi \hat{e}_\phi; \quad (\text{A.13})$$

$$\vec{g} = g_x \hat{i} + g_y \hat{j} + g_z \hat{k} = g_r \hat{e}_r + g_\theta \hat{e}_\theta + g_z \hat{k} = g_r \hat{e}_r + g_\theta \hat{e}_\theta + g_\phi \hat{e}_\phi; \quad (\text{A.14})$$

$$\nabla = \frac{\partial}{\partial x} \hat{i} + \frac{\partial}{\partial y} \hat{j} + \frac{\partial}{\partial z} \hat{k} = \frac{\partial}{\partial r} \hat{e}_r + \frac{1}{r} \frac{\partial}{\partial \theta} \hat{e}_\theta + \frac{\partial}{\partial z} \hat{k} = \frac{\partial}{\partial r} \hat{e}_r + \frac{1}{r} \frac{\partial}{\partial \theta} \hat{e}_\theta + \frac{1}{r \sin \theta} \frac{\partial}{\partial \phi} \hat{e}_\phi; \quad (\text{A.15})$$

$$\vec{I} = \begin{pmatrix} 1 & 0 & 0 \\ 0 & 1 & 0 \\ 0 & 0 & 1 \end{pmatrix} \quad (\text{A.16})$$

for x , y and z the axis and \hat{i} , \hat{j} and \hat{k} the respective unity vectors in Cartesian coordinates, r , θ and z the directions and \hat{e}_r , \hat{e}_θ and \hat{k} the respective unity vectors in cylindrical coordinates and r , θ and ϕ the directions and \hat{e}_r , \hat{e}_θ and \hat{e}_ϕ the respective unity vectors in spherical coordinates.

For one-dimensional forms of flame the formulation for momentum conservation is quite simple. It can be applied to both 1-D planar and spherical systems. Both viscous forces and

gravitational forces are neglected, leaving only those due to pressure acting on the flow. For a given control volume, in a steady-state situation, the sum of all forces acting in a given direction equals the net flow of momentum going out of the control volume in the same direction, as stated by equation A.17

$$\sum F = \dot{m}v_{out} - \dot{m}v_{in}, \quad (\text{A.17})$$

for \dot{m} the mass flux, v_{in} the velocity of the flow entering the control volume and v_{out} the velocity of the flow leaving it. For the forces of pressure P acting on equal surfaces A , equation A.17 can be rewritten as:

$$(PA)_{in} - (PA)_{out} = \dot{m}v_{out} - \dot{m}v_{in}, \quad (\text{A.18})$$

which can be derived by x and divided by the area, giving the taxes for the forces in the following ordinary differential equation:

$$-\frac{dP}{dx} = \dot{m}'' \frac{dv_x}{dx}, \quad (\text{A.19})$$

or, given that $\dot{m}'' = \rho v_x$, being expressed as:

$$-\frac{dP}{dx} = \rho v_x \frac{dv_x}{dx}, \quad (\text{A.20})$$

the one-dimensional form of the Euler equation. Considering a laminar premixed flame, configuration used in the present work, it can be assumed that kinetic energy change across the flame is small, so:

$$\frac{d(v_x^2/2)}{dx} = v_x \frac{dv_x}{dx} \approx 0, \quad (\text{A.21})$$

simplifying the equation for momentum to:

$$\frac{dP}{dx} = 0, \quad (\text{A.22})$$

implying that the pressure is constant through the flow field.

A.4 Energy Conservation

Energy conservation is a thermodynamic concept expressed in the following general equation (Coelho and Costa, 2012):

$$\frac{\partial(\rho h)}{\partial t} + \nabla \cdot (\rho \vec{v} h) = \nabla \cdot \left(\frac{\lambda}{c_p} \nabla h \right) - \nabla \cdot \left[\sum_{i=1}^N \left(1 - \frac{1}{Le_i} \right) \frac{\lambda}{c_p} h_i \nabla y_i \right] + \dot{q}_R''', \quad (\text{A.23})$$

for h the specific enthalpy of the mixture, λ the thermal conductivity, c_p the specific heat of the mixture, while Le_i is the Lewis number, h_i the specific enthalpy and y_i the mass fraction of the i th species; \dot{q}_R''' is the energy generation for volume unit through radiation. The Lewis number is, in general, very close to 1, and is given by the equation:

$$Le = \frac{\lambda}{\rho c_p D^M}, \quad (\text{A.24})$$

for D^M the mass diffusivity.

Simplifying for a unidimensional control volume, it can be represented by the following form of the First Law of Thermodynamics:

$$(\dot{Q}_{in}'' - \dot{Q}_{out}'')A - \dot{W}_{cv} = \dot{m}''A \left[\left(h + \frac{v_x^2}{2} + gz \right)_{out} - \left(h + \frac{v_x^2}{2} + gz \right)_{in} \right], \quad (\text{A.25})$$

for \dot{Q}'' the heat flux as a function of the area A , \dot{W}_{cv} the work produced by the system, \dot{m}'' the mass flux in terms of the area, h the specific enthalpy, v_x the axial velocity, g the gravitational acceleration and z the vertical position. In the cases evaluated in the present work, some considerations are made: (1) steady state, (2) no work done by the control volume, (3) no changes in potential energies. Rearranging, dividing by the area and deriving in relation to x , equation A.25 becomes:

$$-\frac{\dot{Q}_x''}{dx} = \dot{m}'' \left(\frac{dh}{dx} + v_x \frac{dv_x}{dx} \right). \quad (\text{A.26})$$

Assuming there is no radiation, but considering the diffusion and the conduction contribution to the heat flux, its value can be determined as:

$$\dot{Q}_x'' = -k\nabla T + \sum \dot{m}_{i,diff}'' h_i, \quad (\text{A.27})$$

for k the constant for conduction and $\dot{m}_{i,diff}''$ the diffusional flux of the i th species.

The equation A.27 can be derived in relation to x , and equaled to the equation A.26, generating the the final one-dimensional energy conservation equation:

$$\sum \dot{m}_i'' \frac{dh_i}{dx} + \frac{d}{dx} \left(-k \frac{dT}{dx} \right) + \dot{m}'' v_x \frac{dv_x}{dx} = \sum h_i \dot{m}_i'''. \quad (\text{A.28})$$

The further development of this equation is quite complicated, and is available in details in the chapter 7 of the work of Turns (2012). For the applications of the present work, it can be assumed that the Lewis number ($Le = k/\rho c_p D_{AB}$) is equal to 1, an assumption that produces the simplified Shvab-Zeldovich Forms. For a one-dimensional planar flame configuration, neglecting the effects of kinetic energy changes, the following formulation can be produced:

$$\dot{m}'' \frac{d \int c_p dT}{dx} + \frac{d}{dx} \left[-\rho D \frac{d \int c_p dT}{dx} \right] = - \sum h_{f,i}^0 \dot{m}_i''', \quad (\text{A.29})$$

for which the c_p is the specific heat, D the diffusivity of a certain mixture and $h_{f,i}^0$ is the formation enthalpy for the species i . In this equation, the first term represents the rate of sensible enthalpy transported by convection (advection) per unit of volume [W/m^3], the second, the rate of sensible enthalpy transported by diffusion per unit of volume and the third, the rate of sensible enthalpy produced by chemical reaction per unit of volume.

APENDIX B – Tables

B.1 Laminar Flame Speed

Table. B.1: Laminar Flame Speed for Models and Experiments for N-Butanol, $T = 353K$, $p = 1 atm$

Phi	Sarathy <i>et al.</i> (2009)*	Liu <i>et al.</i> (2011)	Zhang <i>et al.</i> (2013)	Model from Sarathy <i>et al.</i> (2009)	Model from Sarathy <i>et al.</i> (2012)	New Model
0.5	X	X	X	7.17	10.32	9.04
0.6	X	X	X	15.51	19.46	17.9
0.7	X	27.85	X	24.17	28.96	27.2
0.8	29.76	36.91	35.4	32.09	37.6	35.74
0.9	36.6	42.95	39.7	38.66	44.63	42.75
1	43.65	47.32	43.9	43.42	49.53	47.68
1.1	47.51	49.33	45.5	45.62	51.65	49.81
1.2	45.19	47.65	45.5	44.64	50.53	48.62
1.3	X	42.62	39.2	39.72	45.44	43.43
1.4	X	33.56	33.4	31.12	36.26	34.5
1.5	X	26.51	25.4	21.65	24.66	24.53
1.6	X	17.11	X	X	X	X

* experiment at $T = 350K$, $p = 0.89 atm$

Table. B.2: Laminar Flame Speed for Models and Experiments for Ethanol, $T = 298K$, $p = 1 \text{ atm}$

Phi	Konnov <i>et al.</i> (2011)	van Lipzig <i>et al.</i> (2011)	Model from Mari- nov (1999)	Model from Konnov <i>et al.</i> (2011)	Model from Sarathy <i>et al.</i> (2012)	New Model
0.50	X	X	7.07	6.08	X	6.17
0.60	X	14.39	15.24	13.56	10.24	13.77
0.70	17.30	22.37	24.08	22.61	17.56	22.41
0.80	26.20	30.43	31.96	31.60	24.75	30.73
0.90	34.50	37.29	38.06	39.36	30.80	37.82
1.00	40.10	42.16	41.88	45.05	35.05	42.98
1.10	42.50	44.29	43.00	48.01	36.96	45.59
1.20	42.00	43.36	40.93	47.51	35.95	44.96
1.30	X	X	35.14	42.80	31.44	40.36
1.40	X	X	X	33.89	23.82	31.86
1.50	X	X	X	23.26	15.28	X
1.60	X	X	X	15.74	X	X
1.70	X	X	X	12.29	X	X

Table. B.3: Laminar Flame Speed for Blends through the scheme from Sarathy *et al.* (2012), $T = 298K$, $p = 1 atm$

Phi	E100	B25	B50	B75	B100
0.50	X	X	5.42	6.12	6.84
0.60	10.24	11.06	11.92	12.83	13.82
0.70	17.56	18.40	19.26	20.19	21.34
0.80	24.75	25.47	26.21	27.07	28.31
0.90	30.80	31.36	31.97	32.74	34.04
1.00	35.05	35.50	35.99	36.68	38.07
1.10	36.96	37.30	37.71	38.35	39.81
1.20	35.95	36.24	36.63	37.26	38.84
1.30	31.44	31.73	32.14	32.80	34.47
1.40	23.82	24.11	24.52	25.16	26.74
1.50	15.28	X	X	X	X

Table. B.4: Laminar Flame Speed for Blends through the new scheme, $T = 298K$, $p = 1 atm$

Phi	E100	B25	B50	B75	B100
0.60	13.77	13.47	13.18	12.90	12.62
0.70	22.41	21.76	21.14	20.54	19.94
0.80	30.73	29.69	28.68	27.71	26.78
0.90	37.82	36.39	35.02	33.70	32.44
1.00	42.98	41.24	39.56	37.96	36.46
1.10	45.58	43.55	41.64	39.84	38.18
1.20	44.96	42.75	40.71	38.82	37.12
1.30	40.36	38.10	36.08	34.24	32.65
1.40	31.86	29.81	28.06	26.50	25.17

B.2 Standard Deviation for Schemes

Standard deviation is a calculated value for the uncertainty of a group of values, given by the formula:

$$\sigma = \sqrt{\frac{\sum_{i=1}^N (S_{L,i} - \bar{S}_L)^2}{N}}, \quad (\text{B.1})$$

where $S_{L,i}$ is the laminar flame speed of a certain scheme at a certain equivalence ratio and \bar{S}_L is its experimental counterpart in a certain experimental work. The square root of the arithmetic mean of difference $(S_{L,i} - \bar{S}_L)^2$, for N equivalence ratios, is the standard deviation.

Tables B.5 and B.6 present calculated values for standard deviation (σ) for schemes evaluated in the present work.

Table. B.5: Standard Deviation for Ethanol Models, in cm/s

	Model from Marinov (1999)	Model from Konnov <i>et al.</i> (2011)	Model from Sarathy <i>et al.</i> (2012)	New Model
Konnov <i>et al.</i> (2011)	4.01	5.26	4.26	3.75
van Lipzig <i>et al.</i> (2011)	1.43	2.56	6.25	0.90
Model from Marinov (1999)		4.01	6.06	2.56
Model from Konnov <i>et al.</i> (2011)			9.08	1.73
Model from Sarathy <i>et al.</i> (2012)				7.33

Table. B.6: Standard Deviation for N-Butanol Models, in cm/s

	Model from Sarathy <i>et al.</i> (2009)	Model from Sarathy <i>et al.</i> (2012)	New Model
Liu <i>et al.</i> (2011)	3.82	2.15	0.98
Sarathy <i>et al.</i> (2009)	1.65	6.42	4.62
Zhang <i>et al.</i> (2013)	2.02	4.63	3.00
Model from Sarathy <i>et al.</i> (2009)		5.14	3.48
Model from Sarathy <i>et al.</i> (2012)			1.70